Iriyama C, Tomita A, Hoshino H, Adachi-Shirahata M, Furukawa-Hibi Y, Yamada K, Kiyoi H, Naoe T.	Using peripheral blood circulating DNAs to detect CpG global methylation status and genetic mutations in patients with myelodysplastic syndrome.	Biochem Biophys Res Commun.	419(4)	662-9	2012

VI. 研究成果の刊行物・別刷

Published November 14, 2011

JEM

Article

Evi1 is essential for hematopoietic stem cell self-renewal, and its expression marks hematopoietic cells with long-term multilineage repopulating activity

Keisuke Kataoka,[1] Tomohiko Sato,[1] Akihide Yoshimi,[1] Susumu Goyama,[1] Takako Tsuruta,[1] Hiroshi Kobayashi,[1] Munetake Shimabe,[1] Shunya Arai,[1] Masahiro Nakagawa,[1] Yoichi Imai,[1] Keiki Kumano,[1] Katsuyoshi Kumagai,[2] Naoto Kubota,[2] Takashi Kadowaki,[2] and Mineo Kurokawa[1]

[1]Department of Hematology and Oncology, [2]Department of Diabetes and Metabolic Diseases, Graduate School of Medicine, University of Tokyo, Bunkyo-ku, Tokyo, 113-8655, Japan

Ecotropic viral integration site 1 (Evi1), a transcription factor of the SET/PR domain protein family, is essential for the maintenance of hematopoietic stem cells (HSCs) in mice and is overexpressed in several myeloid malignancies. Here, we generate reporter mice in which an internal ribosome entry site (IRES)-GFP cassette is knocked-in to the *Evi1* locus. Using these mice, we find that Evi1 is predominantly expressed in long-term HSCs (LT-HSCs) in adult bone marrow, and in the hematopoietic stem/progenitor fraction in the aorta-gonad-mesonephros, placenta, and fetal liver of embryos. In both fetal and adult hematopoietic systems, Evi1 expression marks cells with long-term multilineage repopulating activity. When combined with conventional HSC surface markers, sorting according to Evi1 expression markedly enhances purification of cells with HSC activity. Evi1 heterozygosity leads to marked impairment of the self-renewal capacity of LT-HSCs, whereas overexpression of Evi1 suppresses differentiation and boosts self-renewal activity. Reintroduction of Evi1, but not Mds1-Evi1, rescues the HSC defects caused by Evi1 heterozygosity. Thus, in addition to documenting a specific relationship between Evi1 expression and HSC self-renewal activity, these findings highlight the utility of Evi1-IRES-GFP reporter mice for the identification and sorting of functional HSCs.

CORRESPONDENCE
Mineo Kurokawa:
kurokawa-tky@umin.ac.jp

Abbreviations used: AGM, aorta-gonad-mesonephros; AML, acute myeloid leukemia; BFU-E, burst-forming unit-erythrocyte; CFU-S, CFU-spleen; CLP, common lymphoid progenitor; CMP, common myeloid progenitor; CRA, competitive repopulation assay; EC, endothelial cell; ES, embryonic stem; Evi1, ecotropic viral integration site 1; FL, fetal liver; GEMM, granulocyte/erythrocyte/ macrophage/ megakaryocyte; GM, granulocyte/macrophage; GMP, GM progenitor; HSC, hematopoietic stem cell; HSPC, hematopoietic stem/progenitor cell; IRES, internal ribosome entry site; Lin, lineage; LSK, Lin$^-$ Sca-1$^+$ c-kit$^+$; LT-HSC, long-term HSC; ME, Mds1-Evi1; MEP, megakaryocyte/erythrocyte progenitor; MPP, multipotent progenitor; MSC, mesenchymal stem cell; MSL, Mac-1$^+$ Sca-1$^+$ Lin$^-$; OB, osteoblast; pA, polyadenylation; PB, peripheral blood; RQ-PCR, real-time quantitative PCR; SCF, stem cell factor; ST-HSC, short-term HSC; TPO, thrombopoietin.

Hematopoietic stem cells (HSCs) are distinguished by their inherent capacity to perpetuate themselves through self-renewal and to generate multiple blood cell lineages through differentiation. To maintain a steady-state pool of self-renewing HSCs and prevent HSC exhaustion, these defining properties of HSCs must be tightly regulated. Fine-tuning of stem cell properties requires stem cell–specific expression of their regulatory genes. To elucidate the stemness transcriptional profile, several gene expression microarray analyses have identified quite a few number of HSC-specific gene candidates (Ramalho-Santos et al., 2002; Akashi et al., 2003; Forsberg et al., 2010). However, most of the molecules established to be associated with the regulation of self-renewal capacity in HSCs are widely expressed in the hematopoietic system, and their mutations in genetic models are exclusively accompanied with other hematological abnormalities. Thus, a bona fide stem cell–specific regulator of their function has not been identified, and the functional identification of HSCs based on their ability to self-renew remains difficult.

Ecotropic viral integration site 1 (Evi1) is an oncogenic transcription factor that belongs to the SET/PR domain protein family (Goyama and Kurokawa, 2009). We and others have reported that Evi1 accomplishes an important regulatory function in hematopoietic stem/progenitor

K. Kataoka and T. Sato contributed equally to this paper.

The Rockefeller University Press $30.00
J. Exp. Med. Vol. 208 No. 12 2403-2416
www.jem.org/cgi/doi/10.1084/jem.20110447

Published November 14, 2011

cells (HSPCs) during fetal and adult development. Evi1 expression is limited to HSPCs in the embryonic and adult hematopoietic systems. HSCs in *Evi1*$^{-/-}$ embryos are markedly decreased in numbers with defective repopulating capacity (Yuasa et al., 2005). Moreover, conditional deletion of Evi1 in adult mice revealed that Evi1 is essential for the maintenance of HSCs, but is dispensable for lineage commitment (Goyama et al., 2008). Besides the importance of Evi1 in normal hematopoiesis, dysregulation of Evi1 expression can have distinct oncogenic potential in various myeloid malignancies (Goyama and Kurokawa, 2009). Indeed, aberrant EVI1 expression defines a unique subset of acute myeloid leukemia (AML), and predicts adverse outcome in patients (Lugthart et al., 2008; Gröschel et al., 2010). Furthermore, Evi1 overexpression in hematopoietic cells leads to myelodysplasia in a murine BM transplant model (Buonamici et al., 2004).

In this study, using newly generated Evi1-GFP reporter mice, we demonstrate that Evi1 is preferentially expressed in LT-HSCs, and its expression can mark in vivo long-term multilineage repopulating HSCs and improve the conventional HSC isolation strategy in both adult BM and embryo, which suggests a distinctive relationship between Evi1 and HSC function. Consistent with this, heterozygosity of Evi1 causes a striking reduction in the number of LT-HSCs, with a specific defect of self-renewal capacity caused by accelerated differentiation. Our results point to a potential utility of an Evi1-GFP reporter mouse line for the functional identification of HSCs based on their self-renewal activity, and a central role of Evi1 in regulating the homeostasis of HSCs.

RESULTS

Evi1 is predominantly expressed in LT-HSCs in adult BM

To elucidate Evi1 expression within the hematopoietic system, we have generated gene-targeted mice in which an internal ribosome entry site (IRES)-GFP cassette is knocked-in to the *Evi1* locus by homologous recombination (Fig. 1 A). This knock-in allele functions in a bicistronic manner in that expression of both Evi1 and GFP is under the endogenous transcriptional regulatory elements of the *Evi1* gene, thus enabling us to track Evi1 expression on an individual cell basis. Appropriately targeted TT2 embryonic stem (ES) cell clones were identified by Southern blotting (Fig. 1 B). Mice heterozygous for the *Evi1-IRES-GFP* allele (*Evi1*$^{+/GFP}$) were distinguished from WT mice by genotyping PCR (Fig. 1 C). Western blot analysis showed the presence of GFP protein and comparable expression of Evi1 protein in embryonic fibroblast cells from *Evi1*$^{+/GFP}$ mice compared with WT mice (Fig. 1 D). *Evi1*$^{+/GFP}$ mice were phenotypically indistinguishable in survival, hematopoietic cellularity, and lineage composition from WT controls (unpublished data). Initial flow cytometric analysis of adult *Evi1*$^{+/GFP}$ mice revealed a small, but discrete, population of GFP$^+$ cells (0.15 ± 0.6%; Fig. 2 A), confirming the expression of the *Evi1-IRES-GFP* allele. To examine whether GFP expression levels correlated with those of endogenous *Evi1* mRNA expression, *Evi1* expression of sorted GFP$^-$ and GFP$^+$ cells from BM of *Evi1*$^{+/GFP}$ mice was analyzed by real-time quantitative PCR (RQ-PCR). *Evi1* mRNA was exclusively expressed in the GFP$^+$ cells, and almost no expression was found in the GFP$^-$ cells (Fig. 2 B), indicating that GFP expression in this mouse model faithfully marks cells with active Evi1 expression.

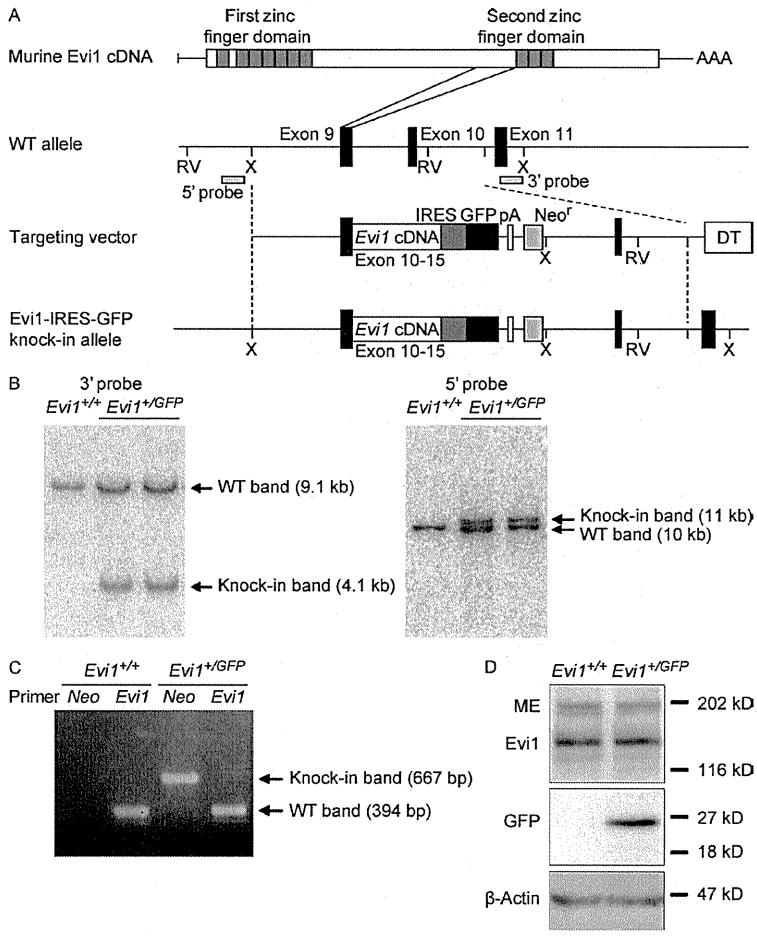

Figure 1. Generation of Evi1-IRES-GFP knock-in mice. (A) The structure of murine *Evi1* and the targeted *Evi1-IRES-GFP* locus is shown. RV, EcoRV; X, XbaI. (B) Southern blot analysis of genomic DNA isolated from WT ES cells (*Evi1*$^{+/+}$) and two independent clones of targeted ES cells (*Evi1*$^{+/GFP}$). DNA was digested with XbaI (left) or EcoRV (right), and hybridized with the indicated probes. (C) Genotyping of *Evi1*$^{+/GFP}$ mice by PCR. (D) Western blot analysis for GFP and Evi1 in embryonic fibroblast cells from *Evi1*$^{+/+}$ and *Evi1*$^{+/GFP}$ mice. β-Actin was used as a loading control. ME, Mds1-Evi1.

Published November 14, 2011

Evi1 mRNA has been shown to be expressed at significantly higher levels in HSPCs (Lin^- $Sca\text{-}1^+$ $c\text{-}kit^+$ [LSK]) and common lymphoid progenitors (CLPs) than in other hematopoietic cells (Yuasa et al., 2005; Chen et al., 2008). To gain insight into the biological function of Evi1 through its cell type–specific expression pattern, the distribution of GFP^+ cells was examined in adult BM from $Evi1^{+/GFP}$ mice. Beyond expectation, GFP expression was highly restricted to the LSK fraction (Fig. 2 A). To confirm stem/progenitor-specific expression of Evi1, we analyzed the GFP fluorescence of various hematopoietic cell populations from BM and spleen of $Evi1^{+/GFP}$ mice. We found a heterogeneous expression of GFP in the LSK fraction, in which about half of the cells were GFP^+ (Fig. 2, C and D). Conversely, only 2.5% of common myeloid progenitors (CMPs) expressed GFP, and almost no expression was found in granulocyte/monocyte progenitors (GMPs) and megakaryocyte/erythrocyte progenitors (MEPs; Fig. 2 C). In contrast to the previous study (Chen et al., 2008), GFP was not expressed in CLPs (Fig. 2 C). In addition, no GFP expression was observed in mature hematopoietic lineages or nonhematopoietic cells in BM (Fig. 2 C). Together, these results suggest that Evi1 is uniquely expressed in HSPCs, but its expression is sharply down-regulated along with differentiation.

Because LSK cells, a population which contains multipotent progenitors (MPPs), short-term HSCs (ST-HSCs), and long-term HSCs (LT-HSCs), include both a GFP^+ fraction and a GFP^- fraction, we next resolved GFP expression within the LSK compartment for other markers characteristic of LT-HSCs. When LSK cells were subdivided according to CD34 and Flk-2 expression (Orford and Scadden, 2008), the $Flk\text{-}2^-$ $CD34^-$ LSK fraction, which is considered to contain most LT-HSC activity, had the highest expression of GFP, and its expression decreased with differentiation to hematopoietic progenitors (Fig. 2 E). In addition, further enrichment for LT-HSCs within the LSK fraction using SLAM family receptors (CD48 and CD150; Kiel et al., 2005) revealed that GFP^+ cells were found in greatest abundance within $CD48^-$ $CD150^+$ LSK cells, in which LT-HSCs are highly enriched. In contrast, GFP expression was substantially down-regulated in $CD48^+$ LSK cells, irrespective of CD150 expression (Fig. 2 F). When we examined how GFP^+ cells were distributed within the LSK fraction, GFP expression was highly enriched in the $Flk\text{-}2^-$ $CD34^-$ LSK or $CD48^-$ $CD150^+$ LSK fractions (Fig. 2, G and H). Therefore, these results indicate that Evi1 is dynamically regulated within HSPCs; its

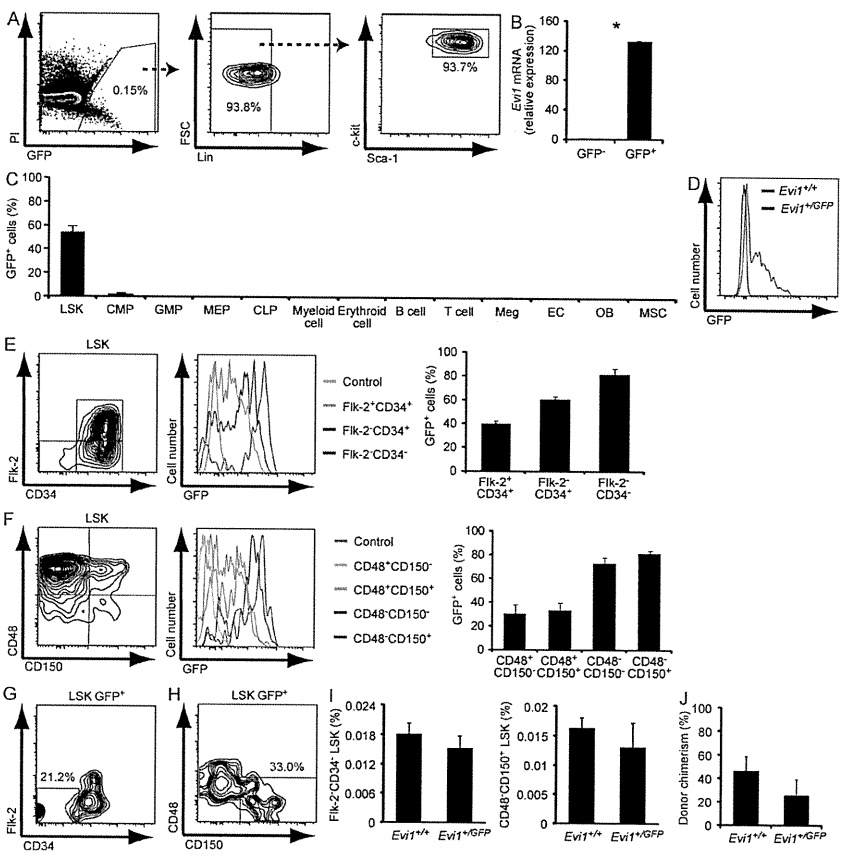

Figure 2. Evi1 is predominantly expressed in LT-HSCs in adult BM. (A) FACS analysis of expression of lineage markers (Lin), c-kit, and Sca-1 on GFP^+ cells in adult BM from $Evi1^{+/GFP}$ mice. Data are representative of three independent experiments. PI, propidium iodide; FSC, forward scatter. (B) RQ-PCR analysis of the expression of *Evi1* mRNA in sorted GFP^- or GFP^+ cells from BM of $Evi1^{+/GFP}$ mice, presented relative to GAPDH expression (*, $P < 0.0001$; $n = 2$). (C) Frequency of GFP^+ cells in indicated BM subpopulation and in splenic T cells from $Evi1^{+/GFP}$ mice ($n = 3$–5). Meg, megakaryocyte; EC, endothelial cell. (D) FACS analysis of expression of GFP in LSK cells from $Evi1^{+/+}$ and $Evi1^{+/GFP}$ mice. Data are representative of at least twenty independent experiments. (E and F) Frequency of GFP^+ cells in subpopulations of LSK cells divided using Flk-2 and CD34 (E) or CD48 and CD150 (F) in $Evi1^{+/GFP}$ mice. (left) Representative plot is shown. (right) Bar graph represents mean ± SD ($n = 3$–4). (G-H) FACS analysis of expression of Flk-2 and CD34 (G) or CD48 and CD150 (H) on LSK GFP^+ cells in BM from $Evi1^{+/GFP}$ mice. Data are representative of two independent experiments. (I) Frequency of $Flk\text{-}2^-$ $CD34^-$ LSK or $CD48^-$ $CD150^+$ LSK cells in BM from $Evi1^{+/+}$ and $Evi1^{+/GFP}$ mice ($n = 3$–5). (J) PB donor chimerism in CRAs, in which 2×10^5 BM cells from $Evi1^{+/+}$ and $Evi1^{+/GFP}$ mice (Ly5.1) were transplanted into lethally irradiated recipients (Ly5.2) together with 2×10^5 competitor BM cells (Ly5.2). Percentages of donor-derived cells (Ly5.1) in PB 16 wk after transplantation are shown ($P = 0.12$; $n = 3$). Data represent mean ± SD.

Published November 14, 2011

expression is predominantly enriched in LT-HSCs and rapidly extinguished during early stages of lineage commitment.

To reinforce Evi1-IRES-GFP knock-in mice as a faithful tool for investigating HSCs, we assessed the number and function of LT-HSCs in BM from *Evi1*$^{+/GFP}$ mice. Flow cytometric analysis revealed that the frequencies of Flk-2$^-$ CD34$^-$ LSK or CD48$^-$ CD150$^+$ LSK cells were comparable between *Evi1*$^{+/+}$ and *Evi1*$^{+/GFP}$ mice (Fig. 2 I). In addition, a competitive repopulation assay (CRA) showed that *Evi1*$^{+/GFP}$ BM cells exhibited slightly less, but not significantly different, long-term reconstitution capacity (Fig. 2 J), indicating that the number and function of HSCs in *Evi1*$^{+/GFP}$ mice are similar to WT controls.

Evi1 expression represents a functionally distinct population that remains in an undifferentiated and quiescent state within HSPCs

As only a subset of LSK cells expressed GFP in *Evi1*$^{+/GFP}$ mice, we hypothesized that Evi1 expression functionally divides the LSK population and marks a more undifferentiated and quiescent state with multipotent differentiation properties in this population. To test this idea, we separated the LSK population into LSK GFP$^-$ and LSK GFP$^+$ cells and compared their biological functions. Initially, we confirmed that LSK GFP$^+$ cells had a much higher level of *Evi1* transcripts than LSK GFP$^-$ cells by RQ-PCR analysis (Fig. 3 A). Interestingly, despite the negative GFP expression, LSK GFP$^-$ cells expressed *Evi1* mRNA at a higher level compared with CMPs and GMPs (Fig. 3 A), which also suggests that Evi1 expression is inversely proportional to the differentiation status. To achieve an estimate of the differentiation stage of these two populations, LSK GFP$^-$ and LSK GFP$^+$ cells were cultured in serum-free medium containing stem cell factor (SCF) and thrombopoietin (TPO). After 3 d of culture, the proportion that remained in the LSK fraction was significantly higher in LSK GFP$^+$ cells than in LSK GFP$^-$ cells (Fig. 3 B), suggesting that LSK GFP$^+$ cells are more primitive HSCs. Next, to evaluate the differentiation potential of LSK GFP$^-$ and LSK GFP$^+$ cells, we performed colony-forming assays in vitro. Although both populations generated an equivalent number of myeloid colonies CFU-granulocyte/macrophage [CFU-GM]), LSK GFP$^+$ cells gave rise to greater numbers of erythroid (burst-forming unit-erythrocyte [BFU-E]) and multipotential (CFU-granulocyte/erythrocyte/macrophage/megakaryocyte [CFU-GEMM]) colonies than LSK GFP$^-$ cells (Fig. 3 C). These data suggest that Evi1 expression correlates with multipotent differentiation capacity. In addition, to assess the colony-forming capacity at the clonal level, single LSK GFP$^-$ and LSK GFP$^+$ cells were cultured in serum-free medium. LSK GFP$^-$ cells formed detectable colonies at a frequency comparable to LSK GFP$^+$ cells, but generated smaller numbers of highly proliferative colonies (>300 cells; Fig. 3 D), indicating that the LSK GFP$^+$ fraction comprises a higher proportion of HSPCs with enhanced proliferative capacity.

Our observations suggested that Evi1 reporter activity is down-regulated as HSCs differentiate. To examine this issue, we forced LSK GFP$^+$ cells to differentiate in vitro in response to SCF, TPO, IL-3, and IL-6. These LSK GFP$^+$ cells predominantly generated GFP$^-$ cells (Fig. 3 E). After culture, the majority of cells that had become GFP$^-$ lost the LSK phenotype, whereas most cells that remained in GFP$^+$ continued to express

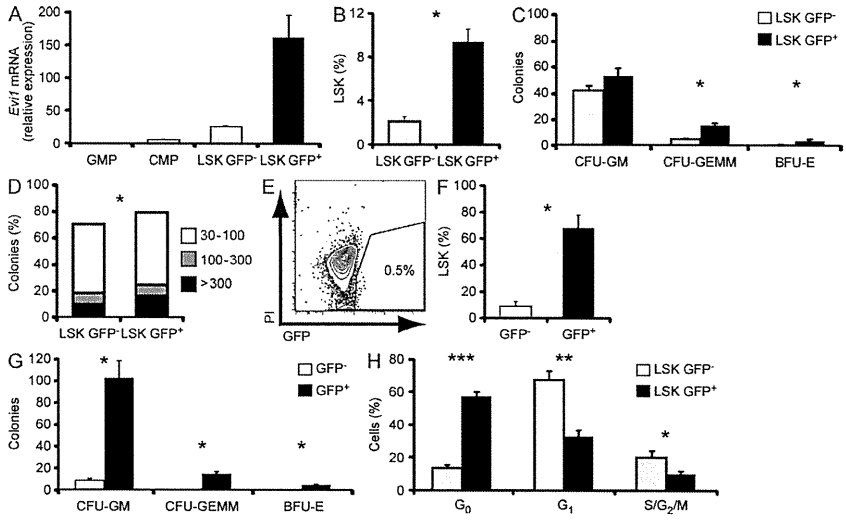

Figure 3. Evi1 expression represents a functionally distinct population that remains in an undifferentiated and quiescent state within HSPCs. (A) RQ-PCR analysis of the expression of *Evi1* mRNA in sorted GMPs, CMPs, LSK GFP$^-$ cells, and LSK GFP$^+$ cells from *Evi1*$^{+/GFP}$ mice, presented relative to *GAPDH* expression ($n = 2$). (B) LSK GFP$^-$ and LSK GFP$^+$ cells were cultured in serum-free medium with 20 ng/ml SCF and 20 ng/ml TPO for 3 d, and the percentage of the remaining LSK fraction was analyzed (*, $P < 0.001$; $n = 3$). (C) Numbers of CFU-GM, CFU-GEMM, and BFU-E colonies derived from 100 sorted LSK GFP$^-$ and LSK GFP$^+$ cells (*, $P < 0.05$; $n = 3$). (D) Single LSK GFP$^-$ and LSK GFP$^+$ cells from *Evi1*$^{+/GFP}$ mice were clone-sorted and cultured in serum-free medium. After 14 d of culture, cell numbers in each colony were analyzed. Their relative distribution is shown (*, $P < 0.05$; $n = 192$ clones from 2 independent experiments). (E) LSK GFP$^+$ cells were cultured in medium containing 10% serum with 50 ng/ml SCF, 50 ng/ml TPO, 10 ng/ml IL-3, and 10 ng/ml IL-6 for 5 d, and the percentage of the remaining GFP$^+$ fraction were analyzed. Data are representative of four independent experiments. (F) The percentages of the remaining LSK fraction in GFP$^-$ and GFP$^+$ cells after culture were analyzed (*, $P < 0.0001$; $n = 4$). (G) Numbers of CFU-GM, CFU-GEMM, and BFU-E colonies derived from 200 GFP$^-$ and GFP$^+$ cells were analyzed (*, $P < 0.0001$; $n = 4$). (H) Cell cycle status of LSK GFP$^-$ and LSK GFP$^+$ cells from *Evi1*$^{+/GFP}$ mice, analyzed by Hoechst 33342 and pyronin Y staining (*, $P < 0.05$; **, $P < 0.005$; ***, $P < 0.0005$, $n = 3$). Data represent mean ± SD.

Published November 14, 2011

the LSK phenotype (Fig. 3 F), indicating that loss of GFP correlates with phenotypic differentiation. To confirm the differential phenotype of the GFP$^-$ and GFP$^+$ cells after culture reflected their functional status, we compared their ability to form colonies in methylcellulose. GFP$^+$ cells yielded significantly more colonies than GFP$^-$ cells (Fig. 3 G), suggesting that functionally primitive HSCs predominantly reside in the GFP$^+$ fraction. Collectively, these data indicate that in vitro culture of LSK GFP$^+$ cells leads to generation of GFP$^-$ cells that are more differentiated, and lend credence to the use of GFP as a fluorescent sensor for the differentiation state of hematopoietic cells.

To determine the cell-cycle distribution of LSK GFP$^-$ and LSK GFP$^+$ cells, we performed Hoechst 33342 and pyronin Y staining, which revealed that the majority of LSK GFP$^+$ cells were in G_0 phase, whereas a significant proportion of LSK GFP$^-$ cells were actively cycling (Fig. 3 H). These data indicate that, within HSPCs, Evi1 expression represents a functionally distinct population that remains in an undifferentiated and quiescent state.

Evi1 expression marks in vivo long-term multilineage repopulating HSCs in adult BM

Based on the aforementioned data, we hypothesized that Evi1 expression would have the potential to effectively mark long-term multilineage repopulating HSCs. To examine this issue, we performed a CRA, in which 500 purified LSK GFP$^-$ or LSK GFP$^+$ cells were transplanted with 2×10^5 competitor BM cells into lethally irradiated recipients (Fig. S1 A). At 16 wk after transplantation, flow cytometric analysis of donor-derived cells revealed long-term reconstitution in all recipients transplanted with LSK GFP$^+$ cells (Fig. 4 A). Moreover, LSK GFP$^+$ cells displayed multilineage potential with robust contribution to myeloid, B, and T cells in peripheral blood (PB) as well as the LSK

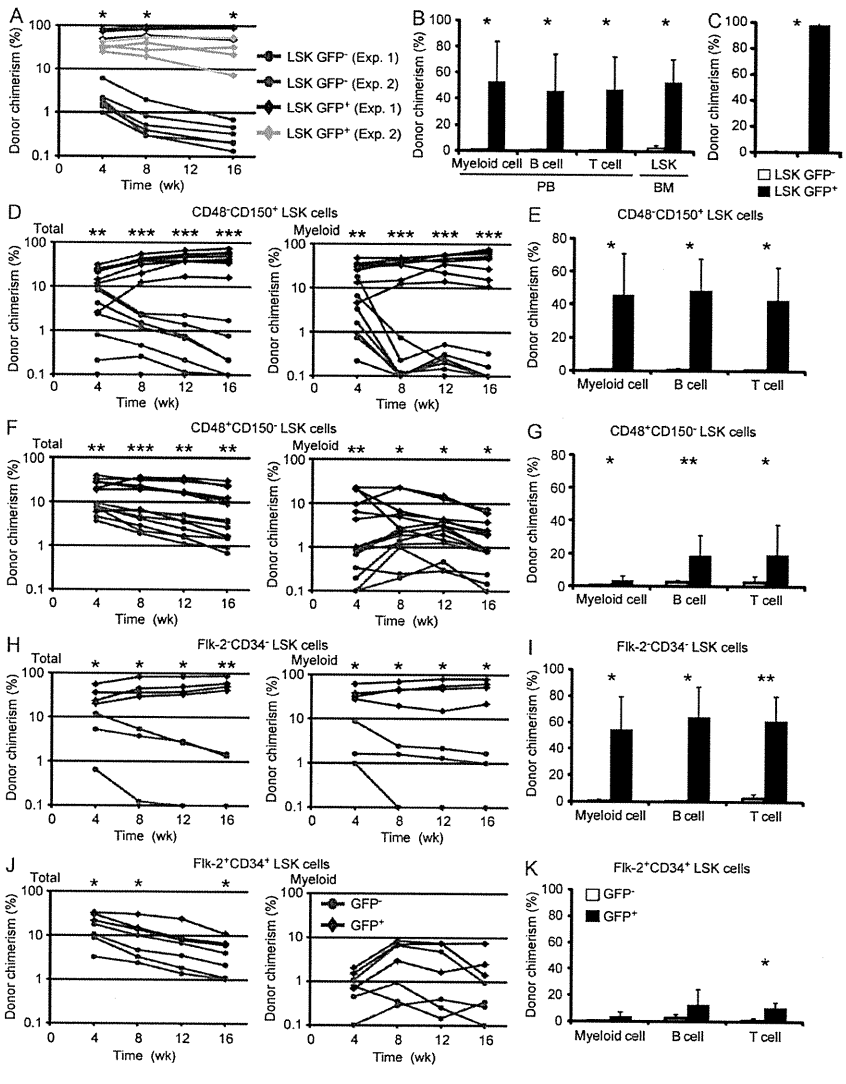

Figure 4. Evi1 expression marks in vivo long-term multilineage repopulating HSCs in adult BM. (A and B) PB donor chimerism in CRAs, in which 500 LSK GFP$^-$ or LSK GFP$^+$ cells sorted from *Evi1*$^{+/GFP}$ mice (Ly5.2) were transplanted into lethally irradiated recipients (Ly5.1) together with 2×10^5 competitor BM cells (Ly5.1 × Ly5.2). (A) Percentages of donor-derived cells (Ly5.2) in PB after transplantation are shown. Each dot indicates an individual recipient mouse (*, $P < 0.005$; $n = 6$–7 from 2 independent experiments). (B) Percentages of donor-derived cells (Ly5.2) in myeloid, B, and T cells of PB and LSK cells of BM 16 wk after transplantation. Recipient mice in experiment 1 were used for the analysis of BM (*, $P < 0.01$; $n = 6$–7 for PB and $n = 3$ for BM). (C) Percentages of donor-derived cells (Ly5.2) in PB of secondary recipient mice (Ly5.1) 16 wk after transplantation. Recipient mice in experiment 1 were used for secondary transplantation (*, $P < 0.0001$, $n = 3$). (D–K) PB donor chimerism in CRAs, in which 100 CD48$^-$ CD150$^+$ LSK GFP$^-$ or CD48$^-$ CD150$^+$ LSK GFP$^+$ cells (D and E; $n = 7$–8), or 500 CD48$^+$ CD150$^-$ LSK GFP$^-$ or CD48$^+$ CD150$^-$ LSK GFP$^+$ cells (F and G; $n = 7$), or 100 Flk-2$^-$ CD34$^-$ LSK GFP$^-$ or Flk-2$^-$ CD34$^-$ LSK GFP$^+$ cells (H and I; $n = 3$–4), or 500 Flk-2$^+$ CD34$^+$ LSK GFP$^-$ or Flk-2$^+$ CD34$^+$ LSK GFP$^+$ cells (J and K; $n = 3$–4) sorted from *Evi1*$^{+/GFP}$ mice (Ly5.1) were transplanted into lethally irradiated recipients (Ly5.2) together with 2×10^5 competitor BM cells (Ly5.2). (D, F, H, and J) Percentages of donor-derived cells (Ly5.1) in total (left) and myeloid cells (right) of PB after transplantation are shown. Each dot indicates an individual recipient mouse (*, $P < 0.05$; **, $P < 0.005$; ***, $P < 0.0005$). (E, G, I, and K) Percentages of donor-derived cells (Ly5.1) in myeloid, B, and T cells of PB 16 wk after transplantation (*, $P < 0.05$; **, $P < 0.005$). Data represent mean ± SD.

Published November 14, 2011

fraction in BM (Fig. 4 B). In contrast, LSK GFP$^-$ cells yielded an almost total inability to generate long-term chimerism (Fig. 4, A and B), which suggests that this population is devoid of self-renewal activity. To confirm the in vivo repopulating capacity of LSK GFP$^+$ cells, we performed secondary transplantation. Similarly, LSK GFP$^+$ cells showed remarkable long-term reconstitution, whereas LSK GFP$^-$ cells consistently failed to produce detectable donor-derived cells (Fig. 4 C), demonstrating that in vivo long-term multilineage repopulating cells are exclusively enriched in the LSK GFP$^+$ fraction in adult BM.

To further refine our analysis designating Evi1 expression as a robust and reliable HSC marker, we compared the repopulating capacity of GFP$^-$ and GFP$^+$ cells within the CD48$^-$ CD150$^+$ LSK fraction, which is enriched for LT-HSCs (Fig. S1 B). Intriguingly, CD48$^-$ CD150$^+$ LSK GFP$^+$ cells exhibited long-term multilineage reconstitution, whereas no engraftment was observed in recipients of CD48$^-$ CD150$^+$ LSK GFP$^-$ cells (Fig. 4, D and E), suggesting that long-term repopulating HSCs predominantly reside in the GFP$^+$ fraction even within the highly subfractionated LT-HSC fraction. We then examined whether Evi1 expression is associated with repopulating capacity in the CD48$^+$ CD150$^-$ LSK fraction, which is enriched for ST-HSCs/MPPs with limited self-renewal activity (Fig. S1 B). Although CD48$^+$ CD150$^-$ LSK GFP$^-$ cells provided only a transient reconstitution, CD48$^+$ CD150$^-$ LSK GFP$^+$ cells showed declining, but sustained engraftment 16 wk after transplantation (Fig. 4 F). In contrast to CD48$^-$ CD150$^+$ LSK GFP$^+$ cells, CD48$^+$ CD150$^-$ LSK GFP$^+$ cells mediated faint myeloid but superior lymphoid reconstitution (Fig. 4, F and G). Although it is controversial whether CD48$^+$ CD150$^-$ LSK cells are transiently reconstituting MPPs/ST-HSCs or lymphoid-biased LT-HSCs with limited long-term engraftment and strong predominance of lymphoid reconstitution (Kiel et al., 2005; Weksberg et al., 2008; Grassinger et al., 2010), Evi1-expressing cells possess higher repopulating capacity within this fraction. When we subfractionated the LSK fraction according to CD34 and Flk-2 expression, and compared the repopulating capacity of GFP$^-$ and GFP$^+$ cells within these subsets (Fig. S1 C), we obtained similar results to the aforementioned findings using SLAM markers (Fig. 4, H–K). These data reveal that, irrespective of the combination of HSC surface markers used, GFP$^+$ cells are the exclusive reservoir of HSC activity, with no reconstitution ability being observed in GFP$^-$ cells within the LT-HSC compartment. Altogether, our results demonstrate that Evi1 expression can further augment the conventional HSC purification strategy, and suggest that Evi1-IRES-GFP knock-in mice allow us to functionally identify HSCs on the ground of self-renewal capacity.

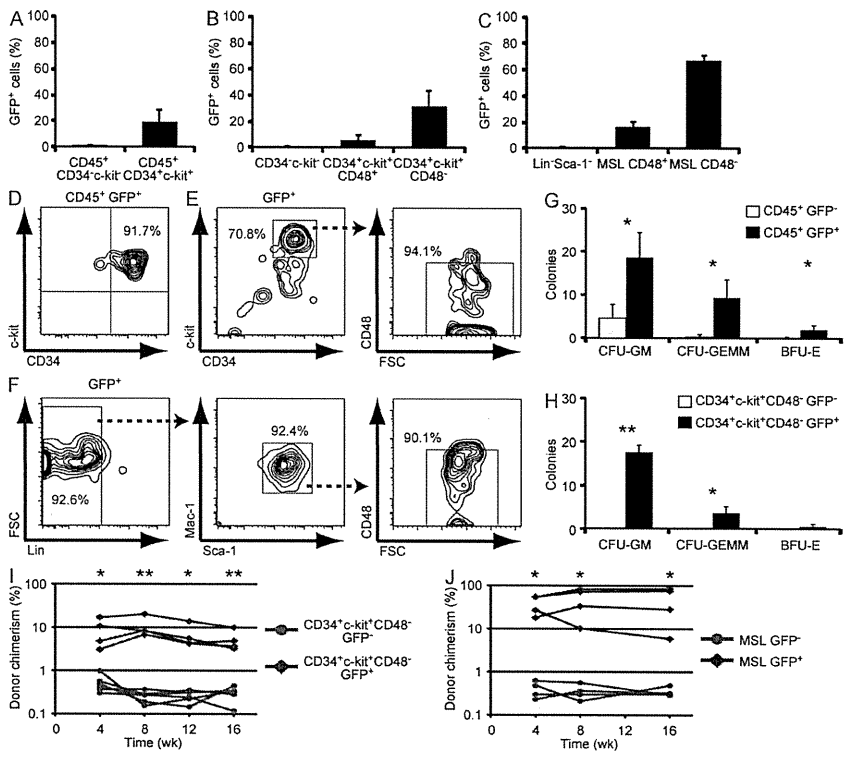

Figure 5. Evi1 expression marks in vivo long-term multilineage repopulating HSCs in embryo. (A–C) Frequency of GFP$^+$ cells in each subpopulation of E10.5 AGM (A; $n = 5$) or E12.5 placenta (B; $n = 3$) or E14.5 FL (C; $n = 5$) from *Evi1*$^{+/GFP}$ embryos. (D–F) FACS analysis of expression of CD34 and c-kit on CD45$^+$ GFP$^+$ cells from E10.5 AGM (D) or CD34, c-kit, and CD48 on GFP$^+$ cells from E12.5 placenta (E) or Lin, Mac-1, Sca-1, and CD48 on GFP$^+$ cells from E14.5 FL (F) in *Evi1*$^{+/GFP}$ embryos. Data are representative of 2 to 10 independent experiments. (G and H) Numbers of CFU-GM, CFU-GEMM, and BFU-E colonies derived from 100 CD45$^+$ GFP$^-$ and CD45$^+$ GFP$^+$ cells sorted from E10.5 AGM (G; $n = 3$), or 100 CD34$^+$ c-kit$^+$ CD48$^-$ GFP$^-$ and CD34$^+$ c-kit$^+$ CD48$^-$ GFP$^+$ cells sorted from E12.5 placenta (H; $n = 3$) in *Evi1*$^{+/GFP}$ embryos (*, $P < 0.05$; **, $P < 0.0005$). (I) PB donor chimerism in CRAs, in which 500 CD34$^+$ c-kit$^+$ CD48$^-$ GFP$^-$ or CD34$^+$ c-kit$^+$ CD48$^-$ GFP$^+$ cells sorted from E12.5 placenta of *Evi1*$^{+/GFP}$ embryos (Ly5.1 × Ly5.2) were transplanted into lethally irradiated recipients (Ly5.2) together with 2 × 10^5 competitor BM cells (Ly5.2). Percentages of donor-derived cells (Ly5.1 × Ly5.2) in PB after transplantation are shown. Each dot indicates an individual recipient mouse (*, $P < 0.05$; **, $P < 0.005$; $n = 4$–6). (J) PB donor chimerism in CRAs, in which 500 MSL GFP$^-$ or MSL GFP$^+$ cells sorted from E14.5 FL of *Evi1*$^{+/GFP}$ embryos (Ly5.2) were transplanted into lethally irradiated recipients (Ly5.1 × Ly5.2) together with 2 × 10^5 competitor BM cells (Ly5.1 × Ly5.2). Percentages of donor-derived cells (Ly5.2) in PB weeks after transplantation are shown. Each dot indicates an individual recipient mouse (*, $P < 0.05$; $n = 4$). Data represent mean ± SD.

Published November 14, 2011

Evi1 expression marks in vivo long-term multilineage repopulating HSCs in embryo

The formation of blood cells begins in the yolk sac of the embryo, and then shifts to the aorta-gonad-mesonephros (AGM) region, and then sequentially to the placenta, fetal liver (FL), and adult BM. There are several major phenotypic and functional differences between fetal and adult HSCs in surface marker profile, cell cycle status, self-renewal potential, gene expression profile, and regulatory mechanism (Mikkola and Orkin, 2006; Orkin and Zon, 2008). Fetal HSCs, in particular, divide rapidly and undergo massive expansion, whereas adult HSCs are mostly quiescent (Bowie et al., 2006). It is known that Evi1 is highly expressed in the yolk sac, paraaortic splanchnopleura, and HSPCs ($CD45^+$ $CD34^+$ c-kit^+) in early embryo (Yuasa et al., 2005). Therefore, we sought to determine whether Evi1 expression can mark fetal HSCs despite their distinct features from adult HSCs, and thus analyzed the expression pattern of GFP in $Evi1^{+/GFP}$ embryos. As expected, GFP expression was highly restricted to HSPCs in the embryonic tissues; $CD45^+$ $CD34^+$ c-kit^+ cells in embryonic day 10.5 (E10.5) AGM, $CD34^+$ c-kit^+ $CD48^-$ cells in E12.5 placenta, and Mac-1^+ Sca-1^+ Lin^- (MSL) $CD48^-$ cells in E14.5 FL (Fig. 5, A-C; Takakura et al., 2000; Kim et al., 2006; McKinney-Freeman et al., 2009). When the distribution of GFP^+ cells in the fetal hematopoietic system was analyzed, most GFP^+ cells exhibited the HSPC-specific marker profile in all embryonic tissues examined (Fig. 5, D–F), indicating the predominant expression of Evi1 in HSPCs during fetal hematopoiesis.

To determine whether Evi1 expression is associated with hematopoietic activity in the embryonic tissues, we performed colony-forming assays in vitro using $CD45^+$ GFP^- and $CD45^+$ GFP^+ cells from E10.5 AGM, and found that $CD45^+$ GFP^+ cells contained almost all colony-forming cells, with few detectable hematopoietic colonies in $CD45^+$ GFP^- cells (Fig. 5 G). In the same manner, within the $CD34^+$ c-kit^+ $CD48^-$ fraction from E12.5 placenta of $Evi1^{+/GFP}$ embryos, colony-forming activity was exclusively present in GFP^+ cells, regardless of colony type (Fig. 5 H). These data suggest that clonogenic hematopoietic progenitors predominantly reside in the Evi1-expressing fraction in fetal hematopoiesis.

To examine whether Evi1 expression would have the potential to effectively mark long-term repopulating HSCs in embryo, we performed a CRA using sorted $CD34^+$ c-kit^+ $CD48^-$ GFP^- and $CD34^+$ c-kit^+ $CD48^-$ GFP^+ cells from E12.5 placenta of $Evi1^{+/GFP}$ embryos (Fig. S2 A). It was obvious that $CD34^+$ c-kit^+ $CD48^-$ GFP^+ cells contributed to the long-term reconstitution of irradiated recipients, whereas donor chimerism was almost undetectable in mice transplanted with $CD34^+$ c-kit^+ $CD48^-$ GFP^- cells (Fig. 5 I), which is in agreement with the results obtained with their adult counterparts. To further assess whether Evi1 expression can enrich long-term repopulating HSCs in embryo, we performed a CRA using purified MSL GFP^- and MSL GFP^+ cells from E14.5 FL (Fig. S2 B). Along with cells in E12.5 placenta, MSL GFP^+ cells gave rise to long-term multilineage reconstitution, whereas no engraftment was observed in recipients of MSL GFP^- cells (Fig. 5 J). These results indicate that fetal HSCs with active *Evi1* transcription exclusively harbor stem cell activity. Collectively, despite the functional differences between fetal and adult HSCs, Evi1 expression marks long-term multilineage repopulating HSCs throughout ontogeny, suggesting a specific relationship between Evi1 expression and HSC self-renewal capacity.

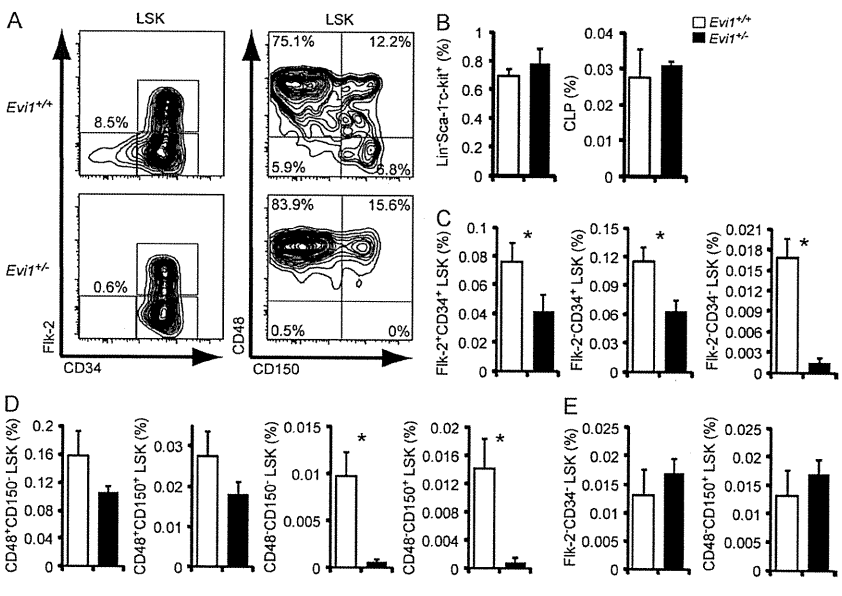

Figure 6. Evi1 heterozygosity leads to an almost complete loss of LT-HSCs in a cell-autonomous manner. (A) FACS analysis of expression of Flk-2 and CD34 or CD48 and CD150 on LSK cells in BM from $Evi1^{+/+}$ and $Evi1^{+/-}$ mice. Data are representative of at least three independent experiments. (B) Frequency of myeloid (Lin^- $Sca\text{-}1^-$ c-kit^+) and lymphoid progenitors (CLPs) in BM from $Evi1^{+/+}$ and $Evi1^{+/-}$ mice ($n = 3$). (C) Frequency of Flk-2^+ $CD34^+$, Flk-2^- $CD34^+$, and Flk-2^- $CD34^-$ subsets within LSK cells in BM from $Evi1^{+/+}$ and $Evi1^{+/-}$ mice (*, $P < 0.0001$; $n = 8$). (D) Frequency of $CD48^+$ $CD150^-$, $CD48^+$ $CD150^+$, $CD48^-$ $CD150^-$, and $CD48^-$ $CD150^+$ subsets within LSK cells in BM from $Evi1^{+/+}$ and $Evi1^{+/-}$ mice (*, $P < 0.01$; $n = 3$). (E) Reciprocal transplantation assay was performed by transplantation of 2×10^5 WT BM cells (Ly5.1) into lethally irradiated $Evi1^{+/+}$ or $Evi1^{+/-}$ mice (Ly5.2). Frequency of Flk-2^- $CD34^-$ LSK or $CD48^-$ $CD150^+$ LSK cells in BM of recipients 16 wk after transplantation is shown ($n = 4$). Data represent mean ± SD.

Published November 14, 2011

Evi1 heterozygosity leads to an almost complete loss of LT-HSCs in a cell-autonomous manner

The aforementioned observations led us to predict that Evi1 plays a functional role specifically in LT-HSCs. To clarify this issue, we analyzed heterozygous *Evi1* KO mice (*Evi1*$^{+/-}$). We previously showed that heterozygosity of Evi1 leads to decreased numbers of LSK and CD34$^-$ LSK cells, as well as impaired long-term repopulating activity (Goyama et al., 2008). In the current study, although Flk-2$^+$ CD34$^+$ and Flk-2$^-$ CD34$^+$ LSK cells were moderately decreased, Flk-2$^-$ CD34$^-$ LSK cells from *Evi1*$^{+/-}$ mice exhibited a marked reduction in frequency compared with WT controls (Fig. 6, A and C). Likewise, when LSK cells were subdivided according to SLAM markers, we observed substantial decreases in CD48$^-$ CD150$^-$ and CD48$^-$ CD150$^+$ LSK subsets (Fig. 6, A and D). Therefore, the number of each subpopulation within the LSK fraction in *Evi1*$^{+/-}$ mice was declined in proportion to their expression level of Evi1, indicating that Evi1 has a dominating effect on the maintenance of LT-HSCs. In contrast, there were no significant differences in BM cellularity and the frequencies of lymphoid and myeloid progenitors, and mature blood cells between *Evi1*$^{+/+}$ and *Evi1*$^{+/-}$ mice (Fig. 6 B and not depicted), indicating that the differentiation potential to all mature lineages and committed progenitors is normal in *Evi1*$^{+/-}$ mice. Collectively, these observations suggest that Evi1 serves as a specific regulator in the earliest stage of adult hematopoietic development.

To exclude the possibility that a defect of BM microenvironment could be responsible for the observed hematopoietic abnormalities in *Evi1*$^{+/-}$ mice, we performed reciprocal transplantation experiments, in which WT BM cells were transplanted into lethally irradiated *Evi1*$^{+/+}$ or *Evi1*$^{+/-}$ mice. At 16 wk after transplantation, flow cytometric analysis showed no differences in the percentages of Flk-2$^-$ CD34$^-$ LSK or CD48$^-$ CD150$^+$ LSK cells in both groups of recipient mice (Fig. 6 E), demonstrating that the profound loss of LT-HSCs in *Evi1*$^{+/-}$ mice is attributed to cell-intrinsic mechanisms.

Evi1 heterozygosity causes specific abrogation of self-renewal capacity in ST- and LT-HSCs

To further characterize which subpopulation in HSPCs is most dependent on Evi1, we purified CD34$^+$ and Flk-2$^-$ CD34$^-$ LSK cells from *Evi1*$^{+/+}$ and *Evi1*$^{+/-}$ mice and compared their differentiation and self-renewal capacity in vitro and in vivo. First, to assess the effect of Evi1 heterozygosity on the biological functions of ST-HSCs/MPPs, we performed colony-forming assays in vitro using *Evi1*$^{+/+}$ and *Evi1*$^{+/-}$ CD34$^+$ LSK cells, which demonstrated no significant differences in the number and type of colonies (Fig. 7 A). Similarly, we found the capacity of *Evi1*$^{+/-}$ CD34$^+$ LSK cells to form colonies in the spleen 11 d after transplantation (CFU-spleen [CFU-S]) was also equivalent to that of WT littermates (Fig. 7 B), indicating Evi1 is dispensable for the regulation of the differentiation and proliferation capacity in ST-HSCs/MPPs. Moreover, to investigate the self-renewal ability of ST-HSCs/MPPs in vivo, we evaluated the short-term repopulating capacity of purified CD34$^+$ LSK cells using a CRA. At 2 wk after transplantation, we detected comparable frequencies of *Evi1*$^{+/+}$ and *Evi1*$^{+/-}$ CD34$^+$ LSK cell–derived myeloid and B cells (Fig. 7 C), suggesting that heterozygosity of Evi1 does not affect the engraftment and differentiation potential of ST-HSCs/MPPs in vivo. However, at later time points in the experiment, we found a moderate but significant decline in the percentage of donor-derived cells from *Evi1*$^{+/-}$ mice (Fig. 7 D). These data indicate that heterozygosity of Evi1 attenuates the self-renewal capacity of ST-HSCs/MPPs, but is not accompanied by any specific differentiation defects in them.

To assess whether Evi1 is required for the functions of LT-HSCs, we compared the self-renewal and proliferation capacity of *Evi1*$^{+/+}$ and *Evi1*$^{+/-}$ Flk-2$^-$ CD34$^-$ LSK cells when cultured in serum-free medium. *Evi1*$^{+/-}$ Flk-2$^-$ CD34$^-$ LSK cells showed comparable proliferation with WT cells for the first week of culture, but thereafter they exhibited pronouncedly impaired growth (Fig. 7 E). After incubation, a significantly lower proportion of cultured *Evi1*$^{+/-}$ Flk-2$^-$ CD34$^-$ LSK cells remained in the LSK fraction than those from *Evi1*$^{+/+}$ mice (Fig. 7 F). In addition, we observed a prominent reduction of hematopoietic colonies contained in cultured *Evi1*$^{+/-}$ Flk-2$^-$ CD34$^-$ LSK cells (Fig. 7 G). Besides, most of the colonies generated from cultured *Evi1*$^{+/-}$ Flk-2$^-$ CD34$^-$ LSK cells consisted of only CFU-GM. These data indicate that heterozygosity of Evi1 results in accelerated loss of HSPCs, leading to the inefficient expansion of their progeny. To evaluate the colony-forming capacity at the single cell level, *Evi1*$^{+/+}$ and *Evi1*$^{+/-}$ Flk-2$^-$ CD34$^-$ LSK cells were clonally sorted and cultured in serum-free medium. Evi1 heterozygosity diminished the colony-forming efficiency of clone-sorted Flk-2$^-$ CD34$^-$ LSK cells, and single *Evi1*$^{+/-}$ Flk-2$^-$ CD34$^-$ LSK cells generated smaller colonies compared with control cells (Fig. 7 H), which indicates that the disruption of Evi1 gene not only decreases the number of clonogenic HSCs but also impairs the functional output per cell.

To assess the repopulating capacity of *Evi1*$^{+/-}$ LT-HSCs in vivo, we performed a CRA using purified Flk-2$^-$ CD34$^-$ LSK cells from *Evi1*$^{+/+}$ and *Evi1*$^{+/-}$ mice. Notably, *Evi1*$^{+/-}$ Flk-2$^-$ CD34$^-$ LSK cells were almost unable to efficiently repopulate all mature lineages as well as stem and progenitor cells 16 wk after transplantation (Fig. 7, I and J), suggesting that LT-HSC function is critically dependent on Evi1 gene dosage. In a noncompetitive setting, although recipients of *Evi1*$^{+/+}$ and *Evi1*$^{+/-}$ Flk-2$^-$ CD34$^-$ LSK cells had similar survival after transplantation (not depicted), *Evi1*$^{+/-}$ Flk-2$^-$ CD34$^-$ LSK cells showed impaired engraftment (Fig. 7 K), suggesting that *Evi1*$^{+/-}$ HSCs were outcompeted by residual host HSCs. However, some of those recipients exhibited long-term multilineage reconstitution (Fig. 7 K and not depicted), confirming that the multipotent differentiation capacity is not abrogated in *Evi1*$^{+/-}$ mice. To further explore the competitive disadvantage of *Evi1*$^{+/-}$ HSCs, we transplanted WT BM cells into unirradiated *Evi1*$^{+/+}$ or *Evi1*$^{+/-}$ mice.

Published November 14, 2011

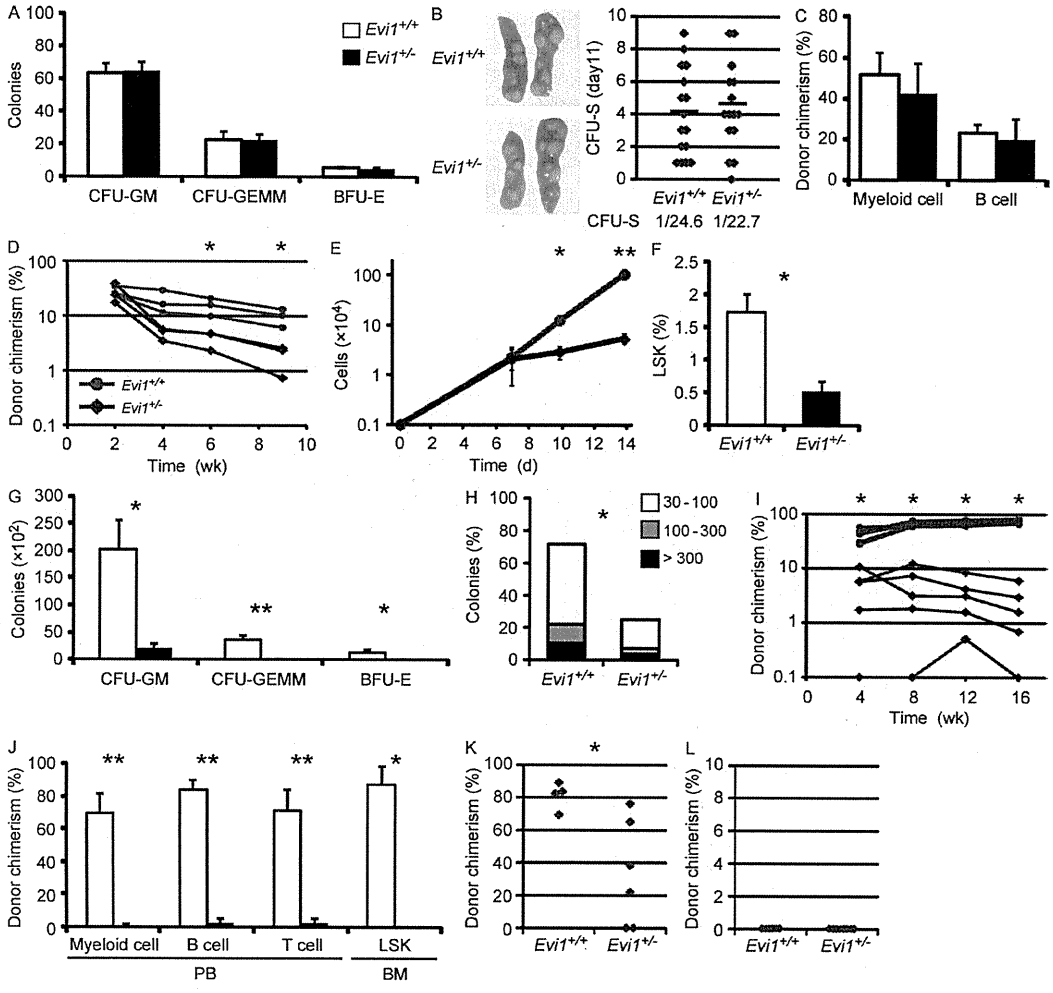

Figure 7. Evi1 heterozygosity causes specific abrogation of self-renewal capacity in ST- and LT-HSCs. (A) Numbers of CFU-GM, CFU-GEMM, and BFU-E colonies derived from 100 sorted *Evi1*$^{+/+}$ and *Evi1*$^{+/-}$ CD34^{+} LSK cells ($n = 3$). (B) Appearance and number of CFU-S colonies in the spleen 11 d after injection of 100 sorted *Evi1*$^{+/+}$ or *Evi1*$^{+/-}$ CD34^{+} LSK cells into lethally irradiated recipients. (left) Representative appearance is shown. (right) Data are shown as a dot plot and each bar represents mean ($n = 15$–16 from 3 independent experiments). (C and D) Short-term in vivo repopulating assay, in which 500 sorted *Evi1*$^{+/+}$ or *Evi1*$^{+/-}$ CD34^{+} LSK cells (Ly5.2) were transplanted into lethally irradiated recipients (Ly5.1) together with 2×10^5 competitor BM cells (Ly5.1). (C) Percentages of donor-derived myeloid and B cells (Ly5.2) in PB 2 wk after transplantation are shown ($n = 3$). (D) Short-term kinetics of the percentages of donor-derived cells (Ly5.2) in PB. Each dot indicates an individual recipient mouse (*, $P < 0.05$; $n = 3$). (E) Proliferation of 1,000 sorted *Evi1*$^{+/+}$ and *Evi1*$^{+/-}$ Flk-2^{-} CD34^{-} LSK cells cultured in serum-free medium supplemented with 20 ng/ml SCF and 20 ng/ml TPO for 14 d (*, $P < 0.01$; ** $P < 0.001$; $n = 3$–4). (F) After 7 d of culture, the percentage of the remaining LSK fraction in cultured *Evi1*$^{+/+}$ and *Evi1*$^{+/-}$ Flk-2^{-} CD34^{-} LSK cells was analyzed (*, $P < 0.005$; $n = 3$). (G) In vitro colony-forming assay was performed to assess the numbers of CFU-GM, CFU-GEMM, and BFU-E colonies after 1,000 *Evi1*$^{+/+}$ and *Evi1*$^{+/-}$ Flk-2^{-} CD34^{-} LSK cells were cultured for 14 d (*, $P < 0.01$; ** $P < 0.001$; $n = 3$–4). (H) Single *Evi1*$^{+/+}$ and *Evi1*$^{+/-}$ Flk-2^{-} CD34^{-} LSK cells were clone-sorted and cultured in serum-free medium. After 14 d of culture, cell numbers in each colony were analyzed. Their relative distribution is shown (*, $P < 0.0001$; $n = 192$ clones from 2 independent experiments). (I–J) Long-term in vivo repopulating assay, in which 200 sorted *Evi1*$^{+/+}$ or *Evi1*$^{+/-}$ Flk-2^{-} CD34^{-} LSK cells (Ly5.2) were transplanted into lethally irradiated recipients (Ly5.1) together with 2×10^5 competitor BM cells (Ly5.1). (I) Percentages of donor-derived cells (Ly5.2) in PB after transplantation are shown. Each dot indicates an individual recipient mouse (*, $P < 0.0001$, $n = 5$–6). (J) Percentages of donor-derived cells (Ly5.2) in myeloid, B, and T cells of PB and LSK cells of BM 16 wk after transplantation (*, $P < 0.001$; ** $P < 0.0001$; $n = 5$–6 for PB and $n = 3$ for BM). (K) Noncompetitive repopulating assay, in which 200 sorted *Evi1*$^{+/+}$ or *Evi1*$^{+/-}$ Flk-2^{-} CD34^{-} LSK cells (Ly5.2) were transplanted into lethally irradiated recipients (Ly5.1) without competitor. Percentages of donor-derived cells (Ly5.2) in PB of recipient mice that survived 12 wk after transplantation are shown (*, $P < 0.05$, $n = 4$–6). (L) Reciprocal transplantation assay was performed by transplantation of 2×10^5 WT BM cells (Ly5.1) into unirradiated *Evi1*$^{+/+}$ or *Evi1*$^{+/-}$ mice (Ly5.2). Percentages of donor-derived cells (Ly5.1) in PB 16 wk after transplantation are shown ($n = 6$–8). Data represent mean ± SD.

Published November 14, 2011

We found no engraftment in both mice (Fig. 7 L), which indicates that the resistance to the donor HSC engraftment during steady-state hematopoiesis is maintained in *Evi1*$^{+/-}$ mice. Collectively, these data suggest that Evi1 is dispensable for the regulation of proliferative and differentiation capacity of ST-HSCs/MPPs, but is strictly required for the maintenance of LT-HSC activity.

To investigate the mechanism behind the impaired HSC activity, we performed cell-cycle and apoptosis assays, but found no differences in the cell-cycle profile or apoptotic rates of Flk-2$^-$ CD34$^-$ LSK cells between *Evi1*$^{+/+}$ and *Evi1*$^{+/-}$ mice (unpublished data). Collectively, in consideration of the accelerated loss of LT-HSC activity in *Evi1*$^{+/-}$ mice, it is supposed that Evi1 heterozygosity directs LT-HSCs from self-renewal toward differentiation to generate more committed progenitors, which is uncoupled from cell-cycle progression or apoptosis.

Forced expression of Evi1 prevents HSPC differentiation and enhances their expansion

The findings noted above led us to hypothesize Evi1 has the potential to inhibit differentiation and enhance HSC self-renewal independent of cell-cycle progression. To clarify this, we adopted a gain-of-function approach, in which WT LSK cells were transduced with Evi1, and then incubated in serum-free medium. Although forced expression of Evi1 gave no apparent growth advantage for the first 10 d of culture, Evi1-transduced LSK cells subsequently manifested a mild but significant increase in proliferation rate (Fig. 8 A). Moreover, we found a substantial increase in the frequency of the remaining LSK fraction in cultured Evi1-transduced cells compared with control cells (Fig. 8 B). In parallel, the number of colonies derived from cultured Evi1-transduced LSK cell was drastically increased (Fig. 8 C). These results suggest that Evi1 activation restricts lineage differentiation and enhances self-renewal activity of HSPCs. Collectively, our data provide compelling evidence that Evi1 regulates the developmental transition from HSPCs to more committed progenitors, suggesting a crucial role of Evi1 in controlling the balance between self-renewal and differentiation.

A recent work suggests that the longer, PR domain-containing isoform Mds1-Evi1 (ME) deficiency alone causes a reduction in the number of HSCs with a loss of long-term repopulation capacity (Zhang et al., 2011). Because both ME and Evi1 are inactivated in our *Evi1* KO model (Goyama et al., 2008), we attempted to genetically dissect the relative roles of ME and Evi1 in maintaining LT-HSCs. For this purpose, we transduced Evi1 or ME into *Evi1*$^{+/-}$ Flk-2$^-$ CD34$^-$ LSK cells and examined whether they could maintain stem cell phenotype after in vitro culture. Reintroduction of Evi1 led to a significant increase in the proportion that remained in the LSK fraction, similar to observations made in *Evi1*$^{+/+}$ cells (Fig. 8 D). However, retroviral transfer of ME was unable to normalize the frequency of the remaining LSK fraction (Fig. 8 D), indicating that Evi1 preferentially rescues *Evi1*$^{+/-}$ LT-HSC defects. Given that ME has broader effects on the hematopoietic system than Evi1 and acts in part by maintaining HSC quiescence through up-regulation of *Cdkn1c* transcription (Zhang et al., 2011), Evi1 and ME may exert their functions in regulating hematopoiesis at different stages and by different mechanisms.

DISCUSSION

In this study, we show that the amount of *Evi1* transcript can be indicative of an undifferentiated state with multipotent differentiation capacity within HSPCs. In both the fetal and adult hematopoietic systems, Evi1 expression can mark long-term multilineage repopulating HSCs, and enhance HSC purification with a combination of other surface markers, suggesting a specific relationship between HSC activity and Evi1 expression throughout ontogeny. This stem cell-specific expression pattern of Evi1 allows us to functionally identify self-renewing HSCs by using Evi1-IRES-GFP knock-in mice, and suggests the relevance of Evi1 in fine-tuning of stem cell properties. Indeed, we provide the genetic evidence confirming that Evi1 has a predominant effect on LT-HSCs by specifically regulating their self-renewal capacity.

The prospective isolation of HSCs is the most important step to dissect their function. The strategy commonly used for HSC isolation is purification based on the expression of a combination of cell surface markers. However, some of these parameters differ between strains of mice, change dramatically during development, and are expressed on many non-HSCs.

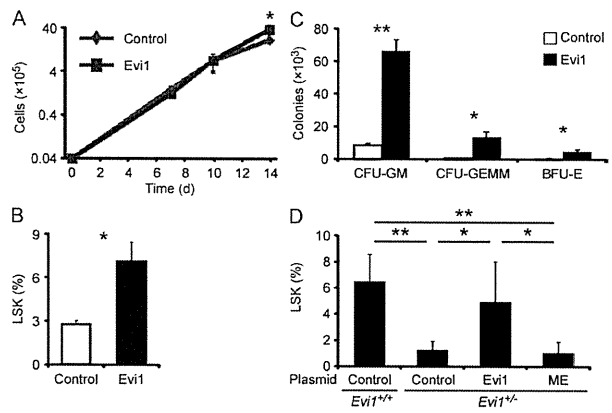

Figure 8. Forced expression of Evi1 prevents HSPC differentiation and promotes their expansion. (A) Proliferation of 3,000 control- or Evi1-transduced LSK cells cultured in serum-free medium with 20 ng/ml SCF and 20 ng/ml TPO for 14 d (*, $P < 0.05$; $n = 3$). (B) After 7 d of culture, the percentage of the remaining LSK fraction in cultured control- or Evi1-transduced LSK cells was analyzed (*, $P < 0.01$; $n = 3$). (C) In vitro colony-forming assay was performed to assess the numbers of CFU-GM, CFU-GEMM, and BFU-E colonies after 3,000 control- or Evi1-transduced LSK cells were cultured for 14 d (*, $P < 0.005$; **, $P < 0.0005$; $n = 3$). (D) Control-, Evi1-, or ME-transduced *Evi1*$^{+/+}$ or *Evi1*$^{+/-}$ Flk-2$^-$ CD34$^-$ LSK cells were cultured in medium containing 10% serum with 50 ng/ml SCF, 50 ng/ml TPO, 10 ng/ml IL-3, and 10 ng/ml IL-6 for 5 d, and the percentages of the remaining LSK fraction were analyzed (*, $P < 0.05$; **, $P < 0.0005$; $n = 5$–6). Data represent mean ± SD.

Published November 14, 2011

Here, we reveal that Evi1 expression specifically correlates with functional HSCs, whereas lack of Evi1 expression exclusively identifies cells without functional HSC activity in both the fetal and adult hematopoietic systems. In particular, Evi1 expression can segregate long-term repopulating HSCs from cells without self-renewal potential even within the highly subfractionated Flk-2$^-$ CD34$^-$ LSK or CD48$^-$ CD150$^+$ LSK compartments. In addition, Evi1-IRES-GFP knock-in mice offer advantages over the conventional HSC surface markers, as the GFP$^-$ and GFP$^+$ subfractions of the Flk-2$^-$ CD34$^-$ LSK or CD48$^-$ CD150$^+$ LSK cells show a quite similar distribution of these markers (unpublished data). Moreover, our findings that Evi1 specifically regulates the self-renewal capacity of HSCs guarantee the potential utility of Evi1 expression as an indicator of HSC activity. Therefore, the Evi1-IRES-GFP knock-in mouse line provides a powerful approach for the functional identification of self-renewing HSCs in vivo, thus opening a new avenue for investigating HSC biology.

Although functional HSCs exclusively reside in the GFP$^+$ population, a proportion of GFP$^+$ cells lack HSC function. As GFP protein is quite stable and degraded more slowly than Evi1 protein (unpublished data), these observations may reflect a remnant of GFP expression from cells that have just differentiated from GFP$^+$ HSCs. However, it is possible that Evi1 expression distinguishes self-renewing ST-HSCs from cells with no self-renewal activity in the ST-HSC/MPP fraction, as Evi1 heterozygosity affects the short-term repopulating capacity of CD34$^+$ LSK cells.

The present findings in the hematopoietic system encourage us to examine the possibility that Evi1 expression serves as a selective marker for stem cells in other tissues or in cancer systems. We show that mesenchymal stem cells (MSCs), one of the few tissue stem cell types that have been established to self-renew in vivo (Morikawa et al., 2009), do not express Evi1. However, a mouse gene expression atlas and prior studies examining the expression pattern of Evi1 in various tissues have reported Evi1 expression in the kidney, ovary, uterus, intestine, stomach, lung, trachea, and nasal cavity in the adult mouse (Morishita et al., 1990; Perkins et al., 1991; Su et al., 2004). It will be interesting to determine, using Evi1-IRES-GFP knock-in mice, whether Evi1-expressing cells in these organs are enriched with tissue stem cells.

Our data suggest a unique association between Evi1 expression and HSC self-renewal activity throughout hematopoietic ontogeny. Along with this stem cell–specific expression pattern of Evi1, the fact that the disruption of a single allele of Evi1 leads to a near total loss of self-renewing HSCs implicates Evi1 as a central regulator in HSC self-renewal. In addition, a recent gene expression profile analysis showed that Evi1 binding sites are enriched in the upstream region of genes expressed selectively in LT-HSCs (Forsberg et al., 2010). In fact, several molecules involved in the regulation of HSC self-renewal have been identified as downstream targets or interacting proteins of Evi1, including Gata2 (Sato et al., 2008; Yuasa et al., 2005), Pbx1 (Shimabe et al., 2009), Runx1 (Senyuk et al., 2007), and TGF-β (Kurokawa et al., 1998). Together with these findings, our data strongly support a model in which Evi1 gene dosage is a critical determinant of HSC self-renewal potential.

Inappropriate expression of EVI1 confers poor prognosis in patients with AML (Lugthart et al., 2008; Gröschel et al., 2010), and therefore improvement of the therapeutic outcome of leukemia with high EVI1 expression is needed. In this study, we reveal that Evi1 overexpression blocks differentiation and induces HSPC expansion. Our data fit with other studies showing that retroviral integration at the *Evi1* locus can be associated with long-term in vivo clonal dominance, occasionally leading to leukemic transformation (Stein et al., 2010). The genetic events underlying AML pathogenesis fall into two groups: (1) mutations that enhance proliferation and survival of hematopoietic progenitors, or (2) mutations that result in impaired differentiation or aberrant acquisition of self-renewal properties of HSPCs (Fröhling et al., 2005). Our data indicate that Evi1 activation can function as the latter mutation and confer enhanced self-renewal capacity in myeloid neoplasms. In addition, we demonstrate that retroviral transfer of Evi1, but not ME, can ameliorate the self-renewal defects in *Evi1*$^{+/-}$ HSCs, highlighting a distinct role of Evi1 in HSC self-renewal. These findings may explain the underlying mechanisms of the clinical observations that, irrespective of ME expression, aberrant EVI1 expression carries an adverse prognostic value in AML (Lugthart et al., 2008, 2010). As it is becoming evident that leukemic stem cells share self-renewal machinery with normal HSCs, the elucidation of how Evi1 controls HSC self-renewal may provide biological insight into the pathogenesis of Evi1-related leukemia.

MATERIALS AND METHODS

Generation of Evi1-IRES-GFP knock-in mice. The targeting construct was assembled in the plasmid vector pBluescript KS. The 5′ arm of the targeting vector consists of a 5.1-kb fragment of BAC clone RP24-481A14 and the 3′ arm consists of a 3.1-kb fragment. The 5′ arm contains *Evi1* intron 8 and exon 9, and the 3′ arm contains intron 9, exon 10, and intron 10. Both arms were obtained by PCR using BAC clone RP24-481A14 as a template, all sequenced, and then inserted into pBluescript KS. Mouse *Evi1* cDNA was isolated from murine embryo cDNA by PCR, with an EcoRI site at the 5′ end and a BamHI site at the 3′ end, which was cloned into pBluescript KS. A 1.3-kb IRES-GFP cassette derived from pGCDNsam-IRES-GFP retroviral vector was inserted downstream of the aforementioned *Evi1* fragment. A polyadenylation (pA) cassette was then ligated 3′ to the IRES-GFP cassette. A neomycin-positive selection (Neo^r) cassette, expressed under control of the PGK promoter, was inserted downstream of the pA cassette. Both pA cassette and loxP-flanked neomycin-positive selection cassette were derived from DT-A/AFP(EGFP)/Neo vector (a gift from the Institute of Physical and Chemical Research Center for Developmental Biology, Kobe, Japan). The partial *Evi1 cDNA-IRES-GFP-pA-loxP-neo* was released intact by digestion with *Sse*8387I and cloned into a unique *Sse*8387I site in exon 9 of BAC arm. A diphtheria toxin–negative selection cassette was cloned into pBluescript KS, 3′ to the targeting construct. The targeting construct was linearized by SacII and transfected into TT2 ES cells by electroporation. Homologous recombinant clones were identified by Southern blot analysis of genomic DNA isolated from individual G418/FIAU-resistant ES cell colonies. The DNA was digested with XbaI, blotted to nylon membranes, and

Published November 14, 2011

hybridized with a 3′ external *Evi1* probe. Confirmatory Southern blotting could detect a 9.1-kb WT *Evi1* allele band and a 4.1-kb correctly targeted *Evi1-IRES-GFP* allele band with this 3′ probe. In EcoRV-digested genomic DNA from positive ES cell clones, a 5′ external probe detected 10- and 11-kb bands from the WT and targeted alleles, respectively. Next, appropriately targeted ES clones were aggregated with 8-cell stage of ICR embryo, and resultant blastocysts were injected into pseudopregnant foster ICR mothers. Chimeric males, which gave germ-line transmission, were crossed with C57BL/6 females. Blastocyst injection and breeding of chimeras were performed in the Animal Center for Biomedical Research, University of Tokyo, Tokyo, Japan.

Mice. Evi1-IRES-GFP knock-in mice were backcrossed onto a C57BL/6 background (Ly5.1 or Ly5.2) for at least four generations (Sankyo-Laboratory Service). Heterozygous *Evi1* KO mice (*Evi1*$^{+/-}$ mice) were previously described (Goyama et al., 2008). C57BL/6-Ly5.1 mice were crossed with Ly5.2 mice to obtain Ly5.1/Ly5.2 mice. Littermates were used as controls in all experiments. All animal experiments were approved by the University of Tokyo Ethics Committee for Animal Experiments and strictly adhered to the guidelines for animal experiments of the University of Tokyo.

Genotype analysis. *Evi1*$^{+/-}$ mice were genotyped by PCR as previously described (Goyama et al., 2008). *Evi1*$^{+/GFP}$ mice were genotyped using a multiplex PCR to detect both WT and *Evi1-IRES-GFP* alleles. Genomic DNA was isolated from tail biopsies and subjected to PCR using *Neo* and *Evi1* primers. PCR with *Neo* primers detects the knock-in allele, and that with *Evi1* primers detects the WT allele. The PCR samples were denatured at 94°C for 2 min, subjected to 30 cycles of amplification (94°C for 30 s, 65°C for 1 min, and 72°C for 1 min), and followed by a final extension step at 72°C. PCR products were resolved by agarose gel electrophoresis. PCR primers are listed below: *Neo* primer forward, 5′-AGGGGATCCGCTGTAAGTCT-3′, reverse, 5′-GCACTGACTGCTCATCCAAA-3′; *Evi1* primer forward, 5′-ATGTCAGCAATTGAGAACATGG-3′, reverse, 5′-ATCCAAAGGTCCTGAGTTCAAA-3′.

Flow cytometry. A list of antibodies is provided in Table S1. Stained cells were sorted with a FACSAriaII, and analysis was performed on LSRII (both from BD). A mixture of antibodies recognizing CD3, CD4, CD8, B220, TER-119, Mac-1, or Gr-1 was used to identify Lin$^+$ cells. Anti-CD127 antibody was added to the lineage mixture, except for the analysis of CLPs. The data analyses were performed with FlowJo software (Tree Star). In experiments with the Evi1-IRES-GFP knock-in mouse, a "fluorescence minus one" littermate control was analyzed in parallel to set GFP gates.

Cell-cycle analyses. For Hoechst 33342 and pyronin Y staining, cells were incubated with 5 ng/ml Hoechst 33342 (Invitrogen) and 25 μg/ml verapamil at 37°C for 45 min. Next, pyronin Y (Sigma-Aldrich) was added to 1 μg/ml, and the cells were incubated for an additional 15 min.

In vitro culture. For in vitro serum-free culture, cells were cultured in StemSpan SFEM (StemCell Technologies) supplemented with 20 ng/ml mouse SCF and 20 ng/ml human TPO, and subsequently subjected to flow cytometry or colony-forming assay at the indicated day after incubation. For colony-forming assay, cells were seeded in duplicate and cultured in cytokine-supplemented methylcellulose medium (MethoCult GF M3434; Stem Cell Technologies). Subsequently, colonies were counted and identified based on morphological examination on day 12. For in vitro differentiation, LSK GFP$^+$ cells were cultured in RPMI-1640 medium (Wako) containing 10% serum with 50 ng/ml mouse SCF, 50 ng/ml human TPO, 10 ng/ml mouse IL-3, and 10 ng/ml human IL-6, and subjected to flow cytometry or colony-forming assay after 5 d of incubation.

Single-cell culture. Cells were clone-sorted into 96-well plates using FACS-based automated cell deposition unit and cultured in StemSpan SFEM supplemented with 20 ng/ml mouse SCF and 20 ng/ml human TPO. After 14 d of culture, cell numbers in each colony were analyzed.

In vivo transplantation assay. Transplantation assays were performed using the Ly5 congenic mouse system. In CRAs, lethally irradiated (9.5 Gy) mice were reconstituted with the indicated subsets from *Evi1*$^{+/+}$, *Evi1*$^{+/GFP}$, or *Evi1*$^{+/-}$ mice, in competition with 2×10^5 unfractionated BM cells from congenic mice. For second BM transplantation, BM cells (1/2 femur equivalent) were obtained from recipient mice 16 wk after transplantation, and transplanted into a second set of lethally irradiated (9.5 Gy) mice. For reciprocal transplantation assays, lethally irradiated (9.5 Gy) or unirradiated *Evi1*$^{+/+}$ and *Evi1*$^{+/-}$ mice were transplanted with 2×10^5 WT BM cells without competitor cells. In non-CRAs, lethally irradiated (9.5 Gy) mice were reconstituted with *Evi1*$^{+/+}$ and *Evi1*$^{+/-}$ Flk-2$^-$ CD34$^-$ LSK cells without competitor cells. Reconstitution of donor-derived cells was monitored by staining PB cells with antibodies against Ly5.1, Ly5.2, CD3, CD4, CD8, B220, Mac-1, and Gr-1. When CD48$^+$ CD150$^-$ LSK cells were transplanted, nonblocking anti-CD48 antibody (MRC OX78 clone) was used (Grassinger et al., 2010).

CFU-S assay. For CFU-S assay, 100 CD34$^+$ LSK cells were injected into lethally irradiated (9.5 Gy) mice. Spleens in transplanted mice were isolated 11 d later, and visually inspected for the presence of macroscopic colonies after fixation in Tellyesniczky's solution.

RQ-PCR. Total RNA was prepared using RNeasy Mini kit (QIAGEN), then cDNA was synthesized with a QuantiTect Reverse Transcription kit (QIAGEN), and used for RQ-PCR with FastStart SYBR Green Master and LightCycler 480 System (Roche Applied Science) according to the manufacturer's instructions. All assays were performed in triplicate and relative expression was normalized to the internal control *GAPDH*. PCR primers are listed below: *GAPDH* primer forward, 5′-CCATCACCATCTTCCAGGAG-3′, reverse, 5′-CCTGCTTCACCACCTTCTTG-3′; *Evi1* primer forward, 5′-ATCGGAAGATCTTAGATGAGTTTTG-3′, reverse, 5′-CTTCCTACATCTGGTTGACTGG-3′

Western blotting. Western blotting was performed as previously described (Goyama et al., 2008). In brief, mouse embryo fibroblast cells were lysed in TNE buffer, subjected to 7% SDS-PAGE, and transferred to a PVDF membrane (Millipore). The blot was incubated with an Evi-1 (C50E12) rabbit monoclonal antibody (Cell Signaling Technology), and visualized by ECL Plus (GE Healthcare).

AGM and placental cell preparation. The day of vaginal plug observation was considered as day 0.5 postcoitum (E0.5). E10.5 AGM region or E12.5 placenta were carefully dissected from embryos, dissociated by incubation with 250 U/ml dispase (Godo Shusei) for 20 min and cell dissociation buffer (Invitrogen) for 20 min at 37°C, and followed by passages through 18–25 G needles. Single cell suspensions were filtered through 70-μm cell strainer and analyzed by flow cytometry.

Endothelial cell (EC), osteoblast (OB), and MSC preparation. After BM cells were flushed out, bones were crushed with a pestle and mortar. Then bone fragments were incubated with a Collagenase/Dispase (1 mg/ml; Roche Applied Science) in MEM α (Wako) with 20% serum and gently agitated for 90 min at 37°C. The dissociated cells were collected, and bone-associated mononuclear cells were isolated with the use of density centrifugation with Histopaque-1083 (Sigma-Aldrich). ECs were defined as CD31$^+$ TER-119$^-$ CD45$^-$, OBs were defined as CD31$^-$ TER-119$^-$ CD45$^-$ Sca-1$^-$ ALCAM$^+$ cells (Nakamura et al., 2010), and MSCs were defined as CD31$^-$ TER-119$^-$ CD45$^-$ Sca-1$^+$ PDGFRα$^+$ cells (Morikawa et al., 2009).

Plasmid construct and retroviral transduction of LSK cells. The murine *Evi1* or *ME* cDNA were inserted into a site upstream of an IRES-EGFP cassette in the retroviral vector pGCDNsam. To produce Evi1-GFP–expressing retrovirus, Plat-E packaging cells were transiently transfected with retroviral constructs by using FuGENE 6 transfection reagent (Roche). LSK cells were purified and incubated in StemSpan SFEM medium and cytokines (100 ng/ml mouse SCF and 100 ng/ml human TPO) for 24 h.

Next, cultured LSK cells were infected with Evi1-GFP retrovirus in the presence of RetroNectin (Takara Bio Inc.). The infected LSK cells were harvested 36 h after retrovirus infection, and GFP$^+$ cells were sorted and subjected to in vitro culture. For retroviral transduction of Evi1 or ME into *Evi1*$^{+/+}$ and *Evi1*$^{+/-}$ Flk-2$^-$ CD34$^-$ LSK cells, those cells were sorted and immediately infected with Evi1- or ME-GFP retroviruses in the presence of RetroNectin. These cells were incubated in RPMI-1640 medium containing 10% serum and cytokines (50 ng/ml mouse SCF, 50 ng/ml human TPO, 10 ng/ml mouse IL-3, and 10 ng/ml human IL-6). After 5 d of culture, the percentage of the remaining LSK fraction in GFP$^+$ cells was analyzed by flow cytometry.

Statistical analysis. Statistical significance of differences between parameters was assessed using a two-tailed unpaired Student's *t* test or Wilcoxon rank sum test.

Online supplemental material. Fig. S1 shows FACS gating strategy used to identify GFP$^+$ population from adult BM of *Evi1*$^{+/GFP}$ mice. Fig. S2 shows FACS gating strategy used to identify GFP$^+$ population from E12.5 placenta or E14.5 FL of *Evi1*$^{+/GFP}$ embryos. Table S1 lists the antibodies used for flow cytometry. Online supplemental material is available at http://www.jem.org/cgi/content/full/jem.20110447/DC1.

We thank T. Kitamura for Plat-E packaging cells; H. Nakauchi and M. Onodera for pGCDNsam-IRES-EGFP retroviral vector; Y. Shimamura, Y. Sawamoto, R. Takizawa, and Y. Oikawa for expert technical assistance; and Institute of Physical and Chemical Research Center for Developmental Biology for DT-A/AFP(EGFP)/Neo plasmid.

This work was supported in part by a Grant-in-Aid for Scientific Research from the Japan Society for the Promotion of Science and by Health and Labour Sciences Research grants from the Ministry of Health, Labour and Welfare. K. Kataoka is a Research Fellow of the Japan Society for the Promotion of Science.

The authors have no conflicting financial interests.

Submitted: 1 March 2011
Accepted: 14 October 2011

REFERENCES

Akashi, K., X. He, J. Chen, H. Iwasaki, C. Niu, B. Steenhard, J. Zhang, J. Haug, and L. Li. 2003. Transcriptional accessibility for genes of multiple tissues and hematopoietic lineages is hierarchically controlled during early hematopoiesis. *Blood.* 101:383–389. http://dx.doi.org/10.1182/blood-2002-06-1780

Bowie, M.B., K.D. McKnight, D.G. Kent, L. McCaffrey, P.A. Hoodless, and C.J. Eaves. 2006. Hematopoietic stem cells proliferate until after birth and show a reversible phase-specific engraftment defect. *J. Clin. Invest.* 116:2808–2816. http://dx.doi.org/10.1172/JCI28310

Buonamici, S., D. Li, Y. Chi, R. Zhao, X. Wang, L. Brace, H. Ni, Y. Saunthararajah, and G. Nucifora. 2004. EVI1 induces myelodysplastic syndrome in mice. *J. Clin. Invest.* 114:713–719.

Chen, W., A.R. Kumar, W.A. Hudson, Q. Li, B. Wu, R.A. Staggs, E.A. Lund, T.N. Sam, and J.H. Kersey. 2008. Malignant transformation initiated by Mll-AF9: gene dosage and critical target cells. *Cancer Cell.* 13:432–440. http://dx.doi.org/10.1016/j.ccr.2008.03.005

Forsberg, E.C., E. Passegué, S.S. Prohaska, A.J. Wagers, M. Koeva, J.M. Stuart, and I.L. Weissman. 2010. Molecular signatures of quiescent, mobilized and leukemia-initiating hematopoietic stem cells. *PLoS ONE.* 5:e8785. http://dx.doi.org/10.1371/journal.pone.0008785

Fröhling, S., C. Scholl, D.G. Gilliland, and R.L. Levine. 2005. Genetics of myeloid malignancies: pathogenetic and clinical implications. *J. Clin. Oncol.* 23:6285–6295. http://dx.doi.org/10.1200/JCO.2005.05.010

Goyama, S., and M. Kurokawa. 2009. Pathogenetic significance of ecotropic viral integration site-1 in hematological malignancies. *Cancer Sci.* 100:990–995. http://dx.doi.org/10.1111/j.1349-7006.2009.01152.x

Goyama, S., G. Yamamoto, M. Shimabe, T. Sato, M. Ichikawa, S. Ogawa, S. Chiba, and M. Kurokawa. 2008. Evi-1 is a critical regulator for hematopoietic stem cells and transformed leukemic cells. *Cell Stem Cell.* 3:207–220. http://dx.doi.org/10.1016/j.stem.2008.06.002

Grassinger, J., D.N. Haylock, B. Williams, G.H. Olsen, and S.K. Nilsson. 2010. Phenotypically identical hemopoietic stem cells isolated from different regions of bone marrow have different biologic potential. *Blood.* 116:3185–3196. http://dx.doi.org/10.1182/blood-2009-12-260703

Gröschel, S., S. Lugthart, R.F. Schlenk, P.J. Valk, K. Eiwen, C. Goudswaard, W.J. van Putten, S. Kayser, L.F. Verdonck, M. Lübbert, et al. 2010. High EVI1 expression predicts outcome in younger adult patients with acute myeloid leukemia and is associated with distinct cytogenetic abnormalities. *J. Clin. Oncol.* 28:2101–2107. http://dx.doi.org/10.1200/JCO.2009.26.0646

Kiel, M.J., O.H. Yilmaz, T. Iwashita, O.H. Yilmaz, C. Terhorst, and S.J. Morrison. 2005. SLAM family receptors distinguish hematopoietic stem and progenitor cells and reveal endothelial niches for stem cells. *Cell.* 121:1109–1121. http://dx.doi.org/10.1016/j.cell.2005.05.026

Kim, I., S. He, O.H. Yilmaz, M.J. Kiel, and S.J. Morrison. 2006. Enhanced purification of fetal liver hematopoietic stem cells using SLAM family receptors. *Blood.* 108:737–744. http://dx.doi.org/10.1182/blood-2005-10-4135

Kurokawa, M., K. Mitani, K. Irie, T. Matsuyama, T. Takahashi, S. Chiba, Y. Yazaki, K. Matsumoto, and H. Hirai. 1998. The oncoprotein Evi-1 represses TGF-beta signalling by inhibiting Smad3. *Nature.* 394:92–96. http://dx.doi.org/10.1038/27945

Lugthart, S., E. van Drunen, Y. van Norden, A. van Hoven, C.A. Erpelinck, P.J. Valk, H.B. Beverloo, B. Löwenberg, and R. Delwel. 2008. High EVI1 levels predict adverse outcome in acute myeloid leukemia: prevalence of EVI1 overexpression and chromosome 3q26 abnormalities underestimated. *Blood.* 111:4329–4337. http://dx.doi.org/10.1182/blood-2007-10-119230

Lugthart, S., S. Gröschel, H.B. Beverloo, S. Kayser, P.J. Valk, S.L. van Zelderen-Bhola, G. Jan Ossenkoppele, E. Vellenga, E. van den Berg-de Ruiter, U. Schanz, et al. 2010. Clinical, molecular, and prognostic significance of WHO type inv(3)(q21q26.2)/t(3;3)(q21;q26.2) and various other 3q abnormalities in acute myeloid leukemia. *J. Clin. Oncol.* 28:3890–3898. http://dx.doi.org/10.1200/JCO.2010.29.2771

McKinney-Freeman, S.L., O. Naveiras, F. Yates, S. Loewer, M. Philitas, M. Curran, P.J. Park, and G.Q. Daley. 2009. Surface antigen phenotypes of hematopoietic stem cells from embryos and murine embryonic stem cells. *Blood.* 114:268–278. http://dx.doi.org/10.1182/blood-2008-12-193888

Mikkola, H.K., and S.H. Orkin. 2006. The journey of developing hematopoietic stem cells. *Development.* 133:3733–3744. http://dx.doi.org/10.1242/dev.02568

Morikawa, S., Y. Mabuchi, Y. Kubota, Y. Nagai, K. Niibe, E. Hiratsu, S. Suzuki, C. Miyauchi-Hara, N. Nagoshi, T. Sunabori, et al. 2009. Prospective identification, isolation, and systemic transplantation of multipotent mesenchymal stem cells in murine bone marrow. *J. Exp. Med.* 206:2483–2496. http://dx.doi.org/10.1084/jem.20091046

Morishita, K., E. Parganas, D.M. Parham, T. Matsugi, and J.N. Ihle. 1990. The Evi-1 zinc finger myeloid transforming gene is normally expressed in the kidney and in developing oocytes. *Oncogene.* 5:1419–1423.

Nakamura, Y., F. Arai, H. Iwasaki, K. Hosokawa, I. Kobayashi, Y. Gomei, Y. Matsumoto, H. Yoshihara, and T. Suda. 2010. Isolation and characterization of endosteal niche cell populations that regulate hematopoietic stem cells. *Blood.* 116:1422–1432. http://dx.doi.org/10.1182/blood-2009-08-239194

Orford, K.W., and D.T. Scadden. 2008. Deconstructing stem cell self-renewal: genetic insights into cell-cycle regulation. *Nat. Rev. Genet.* 9:115–128. http://dx.doi.org/10.1038/nrg2269

Orkin, S.H., and L.I. Zon. 2008. Hematopoiesis: an evolving paradigm for stem cell biology. *Cell.* 132:631–644. http://dx.doi.org/10.1016/j.cell.2008.01.025

Perkins, A.S., J.A. Mercer, N.A. Jenkins, and N.G. Copeland. 1991. Patterns of Evi-1 expression in embryonic and adult tissues suggest that Evi-1 plays an important regulatory role in mouse development. *Development.* 111:479–487.

Ramalho-Santos, M., S. Yoon, Y. Matsuzaki, R.C. Mulligan, and D.A. Melton. 2002. "Stemness": transcriptional profiling of embryonic and adult stem cells. *Science.* 298:597–600. http://dx.doi.org/10.1126/science.1072530

Sato, T., S. Goyama, E. Nitta, M. Takeshita, M. Yoshimi, M. Nakagawa, M. Kawazu, M. Ichikawa, and M. Kurokawa. 2008. Evi-1 promotes

para-aortic splanchnopleural hematopoiesis through up-regulation of GATA-2 and repression of TGF-b signaling. *Cancer Sci.* 99:1407–1413. http://dx.doi.org/10.1111/j.1349-7006.2008.00842.x

Senyuk, V., K.K. Sinha, D. Li, C.R. Rinaldi, S. Yanamandra, and G. Nucifora. 2007. Repression of RUNX1 activity by EVI1: a new role of EVI1 in leukemogenesis. *Cancer Res.* 67:5658–5666. http://dx.doi.org/10.1158/0008-5472.CAN-06-3962

Shimabe, M., S. Goyama, N. Watanabe-Okochi, A. Yoshimi, M. Ichikawa, Y. Imai, and M. Kurokawa. 2009. Pbx1 is a downstream target of Evi-1 in hematopoietic stem/progenitors and leukemic cells. *Oncogene.* 28:4364–4374. http://dx.doi.org/10.1038/onc.2009.288

Stein, S., M.G. Ott, S. Schultze-Strasser, A. Jauch, B. Burwinkel, A. Kinner, M. Schmidt, A. Krämer, J. Schwäble, H. Glimm, et al. 2010. Genomic instability and myelodysplasia with monosomy 7 consequent to EVI1 activation after gene therapy for chronic granulomatous disease. *Nat. Med.* 16:198–204. http://dx.doi.org/10.1038/nm.2088

Su, A.I., T. Wiltshire, S. Batalov, H. Lapp, K.A. Ching, D. Block, J. Zhang, R. Soden, M. Hayakawa, G. Kreiman, et al. 2004. A gene atlas of the mouse and human protein-encoding transcriptomes. *Proc. Natl. Acad. Sci. USA.* 101:6062–6067. http://dx.doi.org/10.1073/pnas.0400782101

Takakura, N., T. Watanabe, S. Suenobu, Y. Yamada, T. Noda, Y. Ito, M. Satake, and T. Suda. 2000. A role for hematopoietic stem cells in promoting angiogenesis. *Cell.* 102:199–209. http://dx.doi.org/10.1016/S0092-8674(00)00025-8

Weksberg, D.C., S.M. Chambers, N.C. Boles, and M.A. Goodell. 2008. CD150- side population cells represent a functionally distinct population of long-term hematopoietic stem cells. *Blood.* 111:2444–2451. http://dx.doi.org/10.1182/blood-2007-09-115006

Yuasa, H., Y. Oike, A. Iwama, I. Nishikata, D. Sugiyama, A. Perkins, M.L. Mucenski, T. Suda, and K. Morishita. 2005. Oncogenic transcription factor Evi1 regulates hematopoietic stem cell proliferation through GATA-2 expression. *EMBO J.* 24:1976–1987. http://dx.doi.org/10.1038/sj.emboj.7600679

Zhang, Y., S. Stehling-Sun, K. Lezon-Geyda, S.C. Juneja, L. Coillard, G. Chatterjee, C.A. Wuertzer, F. Camargo, and A.S. Perkins. 2011. PR domain-containing Mds1-Evi1 is critical for long-term hematopoietic stem cells function. *Blood.* 118:3856–3861.

bjh short report

Deregulated expression of *HMGA2* is implicated in clonal expansion of PIGA deficient cells in paroxysmal nocturnal haemoglobinuria

Yoshiko Murakami,[1,2] Norimitsu Inoue,[3] Tsutomu Shichishima,[4] Rieko Ohta,[1,2] Hideyoshi Noji,[4] Yusuke Maeda,[1,2] Junichi Nishimura,[5] Yuzuru Kanakura[5] and Taroh Kinoshita[1,2]

[1]Department of Immunoregulation, Research Institute for Microbial Diseases, [2]Department of Immunoglycobiology, WPI Immunology Frontier Research Centre, Osaka University, [3]Department of Molecular Genetics, Osaka Medical Centre for Cancer, Osaka, [4]Department of Cardiology and Haematology, Fukushima Medical University, Fukushima, and [5]Department of Haematology and Oncology, Osaka University Graduate School of Medicine, Osaka, Japan

Received 11 July 2011, accepted for publication 16 September 2011

Correspondence: Taroh Kinoshita, PhD, Department of Immunoregulation, Research Institute for Microbial Diseases, Osaka University, 3-1 Yamada-oka, Suita, Osaka 565-0871, Japan.
E-mail: tkinoshi@biken.osaka-u.ac.jp

Summary

Patients with paroxysmal nocturnal haemoglobinuria (PNH) have expanded clonal cells bearing a somatic mutation in the *PIGA* gene. Our previous study on two PNH patients with chromosome 12 rearrangements demonstrated the involvement of *HMGA2* expression in clonal expansion. The present study investigated *HMGA2* expression in PNH patients without chromosomal abnormalities. The expression of short *HMGA2* with latent exon was significantly high in peripheral blood cells from 18 of 24 patients. Over-expression of truncated *HMGA2* in mouse bone marrow cells caused expansion in recipient mice. These results support the idea that deregulated expression of *HMGA2* causes expansion of PNH cells.

Keywords: paroxysmal nocturnal haemoglobinuria, clonal expansion, haemolytic anaemia, haematopoietic stem cell, HMGA2.

Paroxysmal nocturnal haemoglobinuria (PNH) is caused by the somatic mutation of the *PIGA* gene in one or several haematopoietic stem cells followed by their clonal expansion (Takeda *et al*, 1993). We hypothesized a 2-step model of clonal expansion. Step 1 involves the immunological positive selection of glycosylphosphatidylinositol (GPI)-deficient haematopoietic stem cells (Rotoli & Luzzatto, 1989). In this step, GPI-deficient cells proliferate to compensate for anaemia. This may lead to Step 2, where some somatic abnormality occurs in a hyper-proliferating cell resulting in a subclone bearing the growth phenotype. We reported two patients with PNH bearing rearrangements of chromosome 12 unique to PNH clones (Inoue *et al*, 2006). Both had a break in the 3′ untranslated region (UTR) of the same gene, *HMGA2*, which caused it to be expressed ectopically. HMGA2 is an architectural transcription factor physiologically expressed in embryonic tissues. It is known that the fusion of *HMGA2* with other genes results in ectopical expression in many benign mesenchymal tumours, such as lipoma and uterine myoma (Ashar *et al*, 1995). The 3′ UTR of *HMGA2* contains several binding sites of the *MIRLET7*, which regulates both stability of mRNA and translation. Removal of the *MIRLET7* binding sites results in ectopic expression (Mayr *et al*, 2007). Based on these observations, we consider *HMGA2* to be a candidate gene for Step 2, ectopic expression of which causes clonal expansion. In this study, we analysed cells from patients with PNH without chromosomal abnormalities to determine levels of *HMGA2* mRNA by quantitative reverse transcription polymerase chain reaction (RT-PCR). We also checked whether over-expression of HMGA2 in haematopoietic stem cells really causes the clonal expansion using a mouse model.

Patient study

Peripheral blood and bone marrow samples were taken from 25 patients with PNH who had fully expanded PNH clones, namely >50% of granulocytes were CD59 deficient (Table S1). As controls, peripheral blood samples were taken from 11

First published online 24 October 2011
doi:10.1111/j.1365-2141.2011.08914.x

normal volunteers and seven patients with aplastic anaemia, and bone marrow samples were taken from seven normal volunteers. Informed consent was obtained from the patients in accordance with the protocols approved by the Institutional Review Boards of Osaka University Hospital and Fukushima Medical University Hospital.

As cell fractionation procedures drastically decreased the amount of *HMGA2* mRNA and strongly affected the results, whole blood and bone marrow samples were directly taken into PAXgene RNA tubes. RNA was isolated using a PAXgene Blood RNA Kit or PAXgene bone marrow RNA Kit (Qiagen, Hilden, Germany). In addition to the full-size mRNA consisting of exons 1 to 5, termed *HMGA2*a, alternatively spliced short mRNAs, *HMGA2*b, c, d, e, f, *HMGA2*-int4a, b and c, were previously reported (Fig 1A) (Hauke *et al*, 2005). Total transcripts of *HMGA2* were analysed using the primer set located in exons 1 and 2 (black arrow heads, Fig 1A), and TaqMan MGB probe, which spanned the boundary between exons 1 and 2 (Data S1). Full-length transcripts of *HMGA2* were analysed using a TaqMan gene expression assay for HMGA2 (assay ID, Hs00971725_m1, located in exons 4 and 5; grey arrow heads, Fig 1A). *GUSB* was used for the internal control gene (assay ID, Hs00939627_m1). Levels of short transcripts were determined by subtracting normalized expression level of full-length transcript from that of the total transcript. The relative expression was defined as the ratio of normalized expression from each sample to that from the specified normal volunteer (** in Fig 1B).

In the peripheral blood cells, the short transcripts were dominantly expressed in patients with PNH and normal volunteers, and were significantly higher in many of the patients with PNH compared to normal volunteers (Fig 1B). The mean relative expression of the short transcripts was 1·70 ± 1·0 (standard deviation, SD) in patients with PNH and 0·45 ± 0·23 in normal volunteers (Fig S1). Eighteen of 24 PNH patients had short transcript relative expression levels above the mean +2SD of normal volunteers. The splicing variants, *HMGA2*-int4b and c, were cloned from these patients. These results indicate that *HMGA2* was up-regulated in the majority of the patients with PNH bearing fully expanded PNH clones. Seven patients with aplastic anaemia had expression levels similar to normal. In contrast to the peripheral blood cells, the full-length transcript was dominantly expressed in the bone marrow and there was no significant difference in relative expression of *HMGA2* between bone marrow from PNH patients and that from normal volunteers (12·8 ± 3·4 in normal individuals and 12·5 ± 2·5 in patients with PNH, Fig 1C).

Mouse study

A mouse model was used to test whether high expression of *HMGA2* in bone marrow stem cells causes clonal expansion. The human truncated form of *HMGA2* (consisting of the first three exons) was subcloned into the pMYs-IG vector (Kitamura *et al*, 2003). Virus particles encoding HMGA2 and EGFP (pMY-HMGA2-IG), and EGFP only (pMYs-IG) were produced in Plat-E cells and were used to transduce lineage-negative bone marrow cells from mice (C57BL/6, Ly-5·1). Cell aliquots (5×10^5) were intravenously injected into lethally irradiated recipient mice (Ly-5·2). After transplantation, peripheral blood cells of recipient mice were analysed by fluorescence-activated cell sorting to check the percentages of GFP-positive populations in each lineage at the indicated time points (Fig 2A). The efficiency of transduction of bone marrow cells, about 11%, was similar in control and *HMGA2*-transduced groups (Fig 2B). In the two independent experiments, the mice that were transplanted with *HMGA2*-transduced bone marrow cells showed expansion of GFP positive cells in all lineages (Fig 2C). *HMGA2*-transduced myeloid cells seemed to be more drastically expanded than lymphoid cells. These results suggest that expression of truncated *HMGA2* in haematopoietic stem cells caused expansion. We also investigated colony-forming abilities of the *HMGA2*-transduced cells. Mouse bone marrow cells transduced with truncated *HMGA2* generated greater numbers of mixed colonies, suggesting that HMGA2 maintains the pluripotency of stem cells (Fig S2).

Discussion

The expression levels of *HMGA2* were found to be significantly higher in the peripheral blood of many PNH patients compared to normal volunteers (Fig 1B), however, there was no significant difference in the relative expression of *HMGA2* in the bone marrow (Fig 1C). As the bone marrow samples contained various populations of cells, it is possible that the up-regulated expression of *HMGA2* in patients' stem cells might not be detected due to masking by a large number of differentiated cells in the bone marrow that might have similar levels of *HMGA2* expression as normal cells. We speculate that regulation of HMGA2 expression in haematopoieic cells is altered in these patients with PNH and generation of short transcripts is not normally down-regulated in the peripheral blood. *HMGA2* expression is regulated by at least two mechanisms: by transcription factors and by the microRNA, *MIRLET7*. Expression of *MIRLET7B* and *MIRLET7C* was significantly lower in the peripheral blood cells from PNH patients than those from normal volunteers (Fig S3). However, because short transcripts do not contain *MIRLET7* binding sites, lower expression of *MIRLET7B* and *MIRLET7C* does not explain enhanced expression of short transcripts in the peripheral blood cells from PNH patients. Therefore, abnormal increase of short transcripts in the patients is likely to be caused by abnormal induction by some transcriptional factors that up-regulate the total transcripts.

The mouse experiments showed that forced expression of the truncated form of *HMGA2* in stem cells causes clonal expansion. This is consistent with the report that a lentivirally-transduced bone marrow cell clone, which happened to be

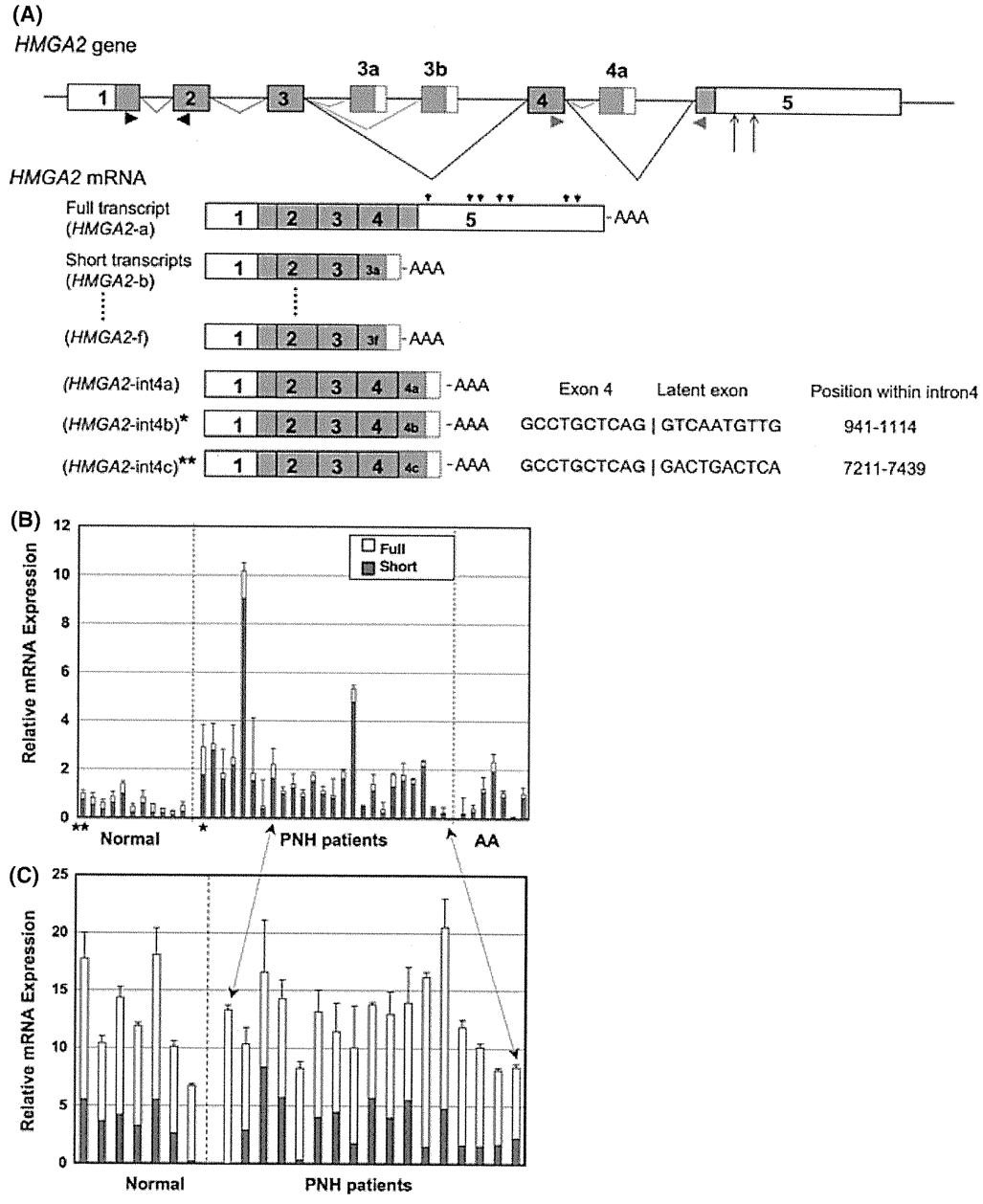

Fig 1. The *HMGA2* gene and its expression in PNH. (A) Structure of the *HMGA2* gene, and its full transcript (*HMGA2*a) and short variants (*HMGA2*b-f and *HMGA2*-int4a–c). 3a, 3b and 4a, latent exons within introns (3c–3f, 4b and 4c are not shown); Black arrowheads, primer pair for amplification of the total transcripts; Grey arrowheads, primer pair for amplification of the full-length transcript; Long arrows, break points in two PNH patients with chromosome 12 rearrangements; Small arrows, binding sites of let-7; * and **, short transcripts cloned from patients' peripheral blood cells showing their sequences of exon 4 to latent exon boundary and positions within intron 4. (B) Relative mRNA expression of *HMGA2* in the peripheral blood cells from PNH patients in comparison with normal volunteers (Normal) and patients with aplastic anaemia or with aplastic anaemia and small PNH clone (AA). White bars, full-length transcript; grey bars, short transcripts; *, the patient with chromosome 12 rearrangement (P1); Relative mRNA expression, a ratio of normalized *HMGA2* mRNA levels in each sample to that in one normal volunteer indicated by **. Data indicate mean + standard deviation in triplicate measurements. Each patient's data is shown in the same order as listed in Table S1 (P1 to P25, PA-1 and PA-2, and AA-1 to AA-5 from left to right). (C) Relative mRNA expression of *HMGA2* in the bone marrow cells from patients with PNH (P8 to P25) in comparison with normal volunteers. White bars, full-length transcripts; grey bars, short transcript; Relative mRNA expression, a ratio of normalized *HMGA2* mRNA levels in each bone marrow sample to that in the peripheral blood cells of one normal volunteer (** in panel B). Arrows with dotted lines, samples within these two arrows are derived from the same patients and correspond to each other in the same order.

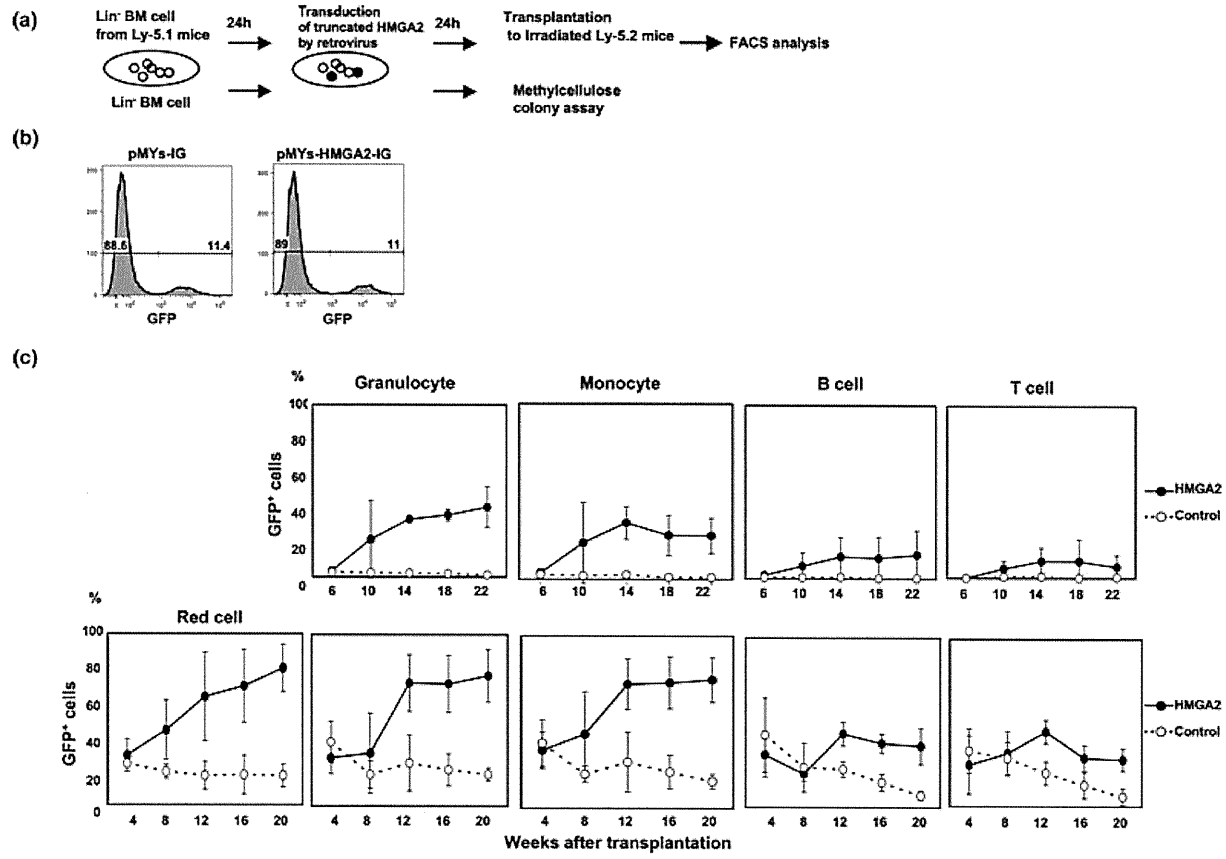

Fig 2. Transplantation of bone marrow cells transduced with HMGA2. (A) The procedure of the experiment. Lineage-negative bone marrow (BM) cells from Ly-5.1 mice were transduced with retrovirus vector bearing truncated HMGA2 and GFP or GFP only as a control, and were transplanted to irradiated Ly-5.2 mice. The peripheral blood cells from the transplanted mice were analysed by fluorescence-activated cell sorting for expression of GFP. The transduced bone marrow cells were cultured in a methylcellulose colony assay. (B) Efficiencies of transduction of bone marrow cells 2 d after retrovirus infection. Percentages of GFP positive cells, indicating the transduction efficiency, were similar in control (pMYs-IG) and HMGA2-transduced (pMYs-HMGA2-IG) groups. (C) Mean percentages of GFP expressing Ly-5.1 positive cells in each lineage of the peripheral blood cells from the transplanted mice at the indicated weeks after transplantation. Black symbols with a line, samples from the mice transduced with truncated HMGA2; White symbols with a dotted line, samples from the control mice transduced with GFP only. Upper (n = 3 in each group) and lower panels (n = 4 in each group) show results of the different sets of experiments.

inserted into intron 3 of *HMGA2*, displayed clonal expansion in gene therapy of a β-thalassemia patient (Cavazzana-Calvo *et al*, 2010). Very recently, it was reported that overexpression of the truncated form of *Hmga2* caused myeloproliferative disease in mice (Ikeda *et al*, 2011). The authors concluded that overexpression of *Hmga2* confers a clonal growth advantage to haematopoietic cells at the level of stem cells. This conclusion is consistent with ours.

The molecular targets of HMGA2 are not clearly known but appear to include cyclin A (Tessari *et al*, 2003), E2F1 transcription factor (Fedele *et al*, 2006), AP1 complex (Vallone *et al*, 1997) and NF-κB (Noro *et al*, 2003). As for the transcriptional regulation of *HMGA2*, TGF-β signalling was reported to regulate its expression (Thuault *et al*, 2006) and growth factors, such as PDGF and EGF-1 were reported to strongly induce *HMGA2* expression in preadipocyte cells via the phosphatidylinositol 3-kinase and mitogen activated protein kinase pathways (Ayoubi *et al*, 1999). However, the molecular mechanisms of deregulated expression of *HMGA2* in patients with PNH still remain to be solved. We predict that some somatic changes induced in GPI-deficient haematopoietic cells cause deregulation of *HMGA2* expression and result in clonal expansion. It is, however, still possible that the observed high expression of *HMGA2* in the peripheral blood cells is not causally related to expansion at the stem cell level. In some patients with PNH, expression of *HMGA2* was not up-regulated in the peripheral blood, so there may be yet other mechanisms that cause clonal expansion.

Acknowledgements

We thank T. Kitamura for the retrovirus vectors and the Plat-E packaging cell, and K. Kinoshita and K. Miyanagi for excellent